12-13-2013 12:00 AM

Methods for Fabricating Printed Electronics with High Conductivity and High Resolution

Tengyuan Zhang
The University of Western Ontario

Supervisor
Jun Yang
The University of Western Ontario

Graduate Program in Mechanical and Materials Engineering
A thesis submitted in partial fulfillment of the requirements for the degree in Master of Engineering Science

METHODS FOR FABRICATING PRINTED ELECTRONICS WITH HIGH CONDUCTIVITY AND HIGH RESOLUTION

(Thesis format: Integrated Article)

by

Tengyuan Zhang

Graduate Program in Mechanical & Materials Engineering

A thesis submitted in partial fulfillment
of the requirements for the degree of
Master of Engineering Science

The School of Graduate and Postdoctoral Studies
The University of Western Ontario
London, Ontario, Canada

Abstract

Flexible and printable electronics are attractive techniques which are believed to be widespread and occupy huge market. However, low conductivity, nozzle clog because of the accumulation of nano-particles and relative high cost (expensive silver/copper nanoparticle inks) limit its appeal. In this thesis, two new effective and convenient methods of fabricating copper patterns with high conductivity and strong adhesion on flexible photopaper and polymer substrates (PET) are demonstrated, solving all those problems. Functional photopaper and PET substrate was prepared with inkjet printing of a palladium salt solution and hyperthermal hydrogen induced cross-linking (HHIC) polyelectrolytes onto its surface respectively, followed by electroless deposition of copper, creating high quality flexible copper patterns on different substrates. The developed technique was successfully applied for fabricating functional flexible circuits such as radio frequency identification devices (RFID) antenna, micro-inductive coil and complex circuit board.

Keywords

Printed electronics, electroless deposition, inkjet printing, screen printing, flexible circuits, low-cost fabrication, high conductivity copper circuits, hyperthermal hydrogen induced cross-linking (HHIC)

Co-Authorship Statement

This master thesis has been prepared according to the regulations for an integrated article format thesis stipulated by the Faculty of Graduate and Postdoctoral Studies at the University of Western Ontario and has been co-authored as follows:

Chapter 2: Fabrication of flexible high resolution copper patterns on photopaper

All the theoretical analyses and experiments were conducted by T. Zhang. A draft of Chapter 2 was prepared by T. Zhang. Dr. Yang and Dr. Wang helped revising the manuscript. Dr. Guo and T. Li got involved in many of our discussions and provided many valuable ideas about this project. A paper entitled ***Fabrication of flexible copper-based electronics with high-resolution and high-conductivity on paper via inkjet printing*** (T. Zhang, X. Wang, and et al.) has been published in the *Journal of Materials Chemistry*, 2013. The patent regarding this technique has been filed.

Chapter 3: Fabrication of flexible high conductivity copper patterns on polymer substrate

All the theoretical analyses were conducted by T. Zhang. All the experiments were conducted by T. Zhang collaborating with Dr. Wang. A draft of Chapter 3 was prepared by T. Zhang. Dr. Wang and Dr. Yang helped revising the manuscript. A paper entitled ***Grafting polyelectrolytes to hydrocarbon surfaces by hyperthermal hydrogen in induced cross-linking for making metallized polymer films*** (X. Wang, T. Zhang, et al.) has been published in Chemical Communication, 2013.

Acknowledgments

First I would like to express my sincere gratitude to my advisor Prof. Jun Yang for his help and continuous support of my master study and research. He not only helped me a lot on courses and experiments but also taught me how to be a qualified researcher, a responsible man for both his work and life. His enthusiasm, patience, diligent, immense knowledge and his ways of doing things are always my guidance in all the time of my study here in Western University.

Besides my advisor, I would like to thank Prof. Xiaolong Wang and Dr. Qiuquan Guo for helping me on my writing work and research. They answered me a lot of questions and trained me for using lots of equipment though they are very busy. My sincere thanks also goes to Dr. Xiaobin Cai, Dr. Peipei Jia, Mr.Zhaoliang Yang, Mr.Luyang Zhang and Mr. Usman Jamil Rajput for the brain storm discussions, for many sleepless nights we were working together before deadlines, also I thank all my friends, for all the fun we have had in the past year.

Last but not the least, I would like to thank my family: my mom and dad for always supporting me in all ways; my girlfriend, Mengmeng Zhang who is always standing by my side sharing all my happiness and sorrow. Without any of you, I would never go this far.

Table of Contents

List of Tables

List of Figures

Preface

Studying in the University of Western Ontario is truly an amazing experience for me. 14 months ago I joined Dr. Yang's group and became a member of the BioNano Technology Lab, 2 months later I started this project and began my journey in the area of the printed electronics. At that time, I never thought that I would publish my own paper and let other people who are also fighting in this area hear my voice. But it finally came true, after all those days and nights spent in the lab, fighting shoulder to shoulder with my fellow scientists and colleagues, the hope for good results, the disappointment of each failed attempt and the joy of weekends.

I always consider myself as a lucky dog, and this time will be no exception. I feel lucky to have the opportunity to follow Dr. Yang, who is an amazing supervisor, for my master degree and contribute as a member in his group. We always say that a good teacher should not only propagate the doctrine, impart professional knowledge, but also should resolve doubts. Well, Dr. Yang did all of them, he is not only our research leader but also our mentor in life. He taught me how to do the research, and what's more, he also helped me to find out why I should do that, which I think is more important. In Dr. Yang's group, you are not alone, because we work together, solve each problem together and share the joy of success together.

Time is always flying and efforts will make the past days become memorable. I treasure all the people who ever helped me and are supporting me.

This thesis is dedicated to all of you.

Chapter 1

1 Introduction

1.1 Research motivation

Flexible electronics/devices, which can maintain functionality when subject to a large deformation or stress, represent an important direction of future electronics manufacturing and mechanical engineering. Wearable, rollable and foldable displays, sensors, solar cells, batteries and other flexible electronics/devices will bring us completely different user experience and even change our daily life. For example, wearable or implantable biomedical devices can be the next generation tools for heath monitoring, disease diagnostics and treatment. Several strategies have been developed to make flexible and stretchable electronics/devices. For example, one approach is to use organic conductive or semiconducting materials, or inorganic thin films or one-dimensional nanomaterial that can flex. Another approach is to integrate conventional high-performance silicon based electronic components with optimized structural configurations such as wavy shapes that can absorb the induced deformation. A lot of effort has also been focused on the fabrication of flexible electrical circuits that can be stretched, twisted or compressed. When functional components such as light emitting diodes (LEDs) connected and powered by such circuit are bended, twisted and compressed the circuits deform to offer the flexibility allowance of the whole device while the central functioning components are in fact subject to very small stress.

However many of these studies are still in infancy and mostly rely on sophisticated and expensive nano/micro fabrication processes and facilities, and involve high processing

temperatures and toxic wastes. It is therefore highly desirable, yet extremely challenging, to develop low-cost and scalable facile methods that can operate at low processing temperatures and use inexpensive materials to make integratable, flexible or even stretchable electronics and devices.

Recently, several printing techniques, including inkjet printing, nanoimprinting and screen printing, have emerged as a very promising technical trend to produce flexible and stretchable electronics/devices. Especially for the material or inkjet printing as an additive manufacturing method, it has proved to be very versatile and cost-effective for making flexible and stretchable electronics via a direct writing manner with merits of high efficiency, low material consumption and programmable control. However challenges remain in low conductivity of printed circuits, instable printing due to nozzle clog and misdirection jetting, weak adhesion between the printed materials and the substrates, low resolution, limited choices of substrate materials, and relatively high cost due to the use of Ag or Au nanoparticle based conductive inks. Particularly the low conductivity and instable printing problems directly affect the quality control during the manufacturing, and performance and lifetime of the devices, causing fatal functional failure of the printed circuits or devices. If the printing resolution can be improved, cost and material consumption will be reduced, throughput will be further increased, and many more applications will become available.

There is increasing demand for high quality and low cost electronic components such as RFID tags, thin film transistor, super capacitor, flexible sensor and devices, which require innovative fabrication techniques that are faster but cheaper compared to traditional production methods. [1-3] It is also predicted that the market of flexible

organic and printed electronics will exceed $300 billion by 2028. [4] So a new generation technique of fabricating flexible printed electronics which can overcome all those problems mentioned above in badly need.

This thesis presents a new developed ultra-low-cost method of inkjet printing combined with electroless deposition (ELD) process to prepare high-resolution high-conductivity copper patterns on flexible photopaper substrate, overcoming almost all the problems that the industry of printed electronics is facing today

1.2 Background and literature review

It has been demonstrated that flexible or stretchable printed electronics/devices are opening up many exciting opportunities, [5, 6] such as wearable electronics, [7] skin sensors [8, 9] and biological actuators etc. [10] The key to realize flexibility or stretchability of electronics/devices is the integration of excellent mechanical robustness with electrical/electronic performance. Rigid materials like silicon may exhibit good electrical/electronic performance and stability, but have poor mechanical ductility. On the other hand, soft materials show excellent mechanical deformability while having unsatisfactory electrical and electronic properties. And it is almost impossible for the conventional manufacturing process to fabricate electronics on flexible or stretchable substrate such as PET, PI, photopaper and PDMS.

Several strategies have been suggested to address the challenges. For example, one can configure conductive thin films or ribbons into in-plane waves or out-of-plane buckles and then bond onto polymeric substrates to realize flexible electronics/devices. Various flexible electronic devices have been developed by using the buckled, serpentine

structures of silicon or metals as interconnects or electrodes. [11-13] Although flexibility and even stretchability up to 70% strain have been achieved, the drawback of this strategy is the complicated micro/nanofabrication processes. Another strategy, filling polymeric or rubbery matrix with conductive materials, is a less-costly method to make flexible and stretchable conductive composites. The conductive materials can be metals, [14, 15] conductive polymers [16] and carbon materials. [17-21] Although this strategy can easily yield flexible conductors and electronics, the disadvantages are also obvious including low conductivity and the change of conductivity under stress. The normal trend is that the conductivity decreases under bending. However non-monotonic piezoresistive behavior, which is counter-intuitive, has also been observed in many conductive polymer nanocomposites. [22-24] Under stretching or other types of mechanical deformation, the conductive fillers behave differently from the polymer phase in terms of mechanical responses. This induces re-distribution and/or re-orientation of nanofiller, deboning or rebonding at nanofiller-polymer interfaces. Consequently, electron transport mechanisms, including conducting path mechanism and electron hopping or tunneling effect, are significantly changed, leading to the change of the conductive properties of the nanocomposites. This mechanism is complex and has not yet been fully understood. Therefore the quality control becomes difficult if the electronics/devices are made based on this strategy.

Conventional electronic fabrication systems are mostly based on photolithography, a complex and time-consuming process that involves large volumes of hazardous waste and expensive facilities, what' more, it cannot be used for fabricating electronics on various substrate especially those flexible, easy corrosion but environmental friendly

substrates. In this regard, the strategy of coating conductive materials onto polymers or elastomers, has emerged as a very promising method, which enables fabrication of flexible or stretchable electronics in a low-cost and scalable manner. [25-28] Various technologies have been emerged as promising technical trends to produce flexible electronics and devices including spray coating, [25] physical deposition, [26, 27] chemical deposition, inkjet printing, [29] non-vacuum deposition, [30] screen printing etc. [31] Among these, inkjet printing technology has gained more and more attention in recent years for its appeal of low-cost, non-contact, scale-up capability, low material and energy consumption, programmable control and maskless additive manufacturing. Various flexible and stretchable electronics have been inkjet printed in a laboratory setting using carbon nanomaterial, [32, 33] conductive polymers, [34] metal nanoparticles [35] and liquid metals. [36] Due to its versatility and cost-effectiveness, inkjet printing has become one of the most promising methods for fabrication of flexible and stretchable electronics.

However delamination or peeling-off is always a concern because the conductive materials are typically deposited on the top of substrates only. The possibility of failure under repeated mechanical loading limits its applications in areas where reliability and stability are important. In addition, unsatisfactory conductivity of printed materials that is far below that of the bulk material is another major problem. Applied to printed electronics based on inkjet printing, most of the research efforts are focused on direct printing of metal nanoparticles or conductive polymer, followed by sintering to make them conductive. Copper or silver nanoparticle based inks were commonly printed on a treated PET/PI substrate, with a nozzle size of larger than 15 μm, and

dimension of the final resulted metal pattern is normally around 10-20 μm, five times better than the current resolution of screen printing. However, clogging is always a common critical issue for micron size nozzles due to the accumulation of nanoparticles at the nozzle opening caused by interactive force. Other critical issues reside in the oxidization and sedimentation stability of the corresponding inks, generally requiring large amounts of stabling and decoration agent and is thus in a very low concentration of metal particles which consequently leads to a high resistance of the printed patterns. [37, 38] Extensive research and development are required to overcome these technical hurdles to advance the material printing technology to the state of the art manufacturing process. For example, how to improve conductivity and resolution of printed circuits, improve adhesion between the printed materials and the substrates, further reduce the cost, and enrich choices of substrate materials, are all key issues that remain to be solved. Thus it's strategically important to develop robust, high-resolution, high-performance and low-cost material printing technologies, which enable a broader variety of substrate materials, good electrical and electronic performance close to conventional electronics, and the use of inexpensive metals like copper.

1.3 Research objectives

The main purpose of our research is to develop new techniques that present competitive advantages over nowadays printed electronics fabrication technologies in terms of conductivity, resolution, material-substrate adhesion and variety of choices of substrates. We are aiming at pushing forward the board of the printed electronics industry, solving the problems of printed electronics fabrication that we are facing today. We believe that the printed electronics will completely replace conventional PCB fabrication technology

if some of the technical issues were solved. So we started this work, trying to make our own contributions to the development of human technology.

1.3.1 Objective 1: Developing a new method to fabricate printed electronics solving several critical issues

The most common printed electronics fabrication technology is to inkjet print Ag-nanoparticle or Cu-nanoparticle based inks, where the nozzle size is typically larger than 10 μm, and the line and space dimension is normally around 10 μm and 20 μm, respectively. The nozzle size is one of key factors that determine the resolution of inkjet printing. Ideally the smaller the nozzle size, the higher the printing resolution. However clogging is always a common issue for micron size nozzles due to accumulation of nanoparticles at the nozzle opening. Ag inks are popular mainly because they are stable and sintering of Ag nanoparticles can take place at low temperature around 150 ºC. However Ag is still relatively expensive compared to Cu. Our goal is to print inexpensive metals like Cu with good conductivity and with high printing resolution. Here we propose to print catalyst (noble-metal-containing salt) solution instead of conductive inks which are a complex mixture of nanoparticles, stabling agent, solvent and other additives. Printing pure catalyst noble-metal-containing salt solution eliminates the issue of nozzle blocking and allows us to use smaller and even nanometer scale printer head nozzle to greatly improve the printing resolution. Therefore the new approach offers a promise to achieve a breakthrough printing resolution. After printing catalyst, the substrate is immersed in Cu salt solution and electroless deposition will occur to deposit Cu nanoparticles on the substrate according to the printed patterns.

Effects of concentration of the palladium salt on the viscosity and surface tension of the ink, effects of ELD time on the surface morphology and conductivity will be investigated. Jetting program of material printers like the voltage control waveform, jetting frequency, meniscus vacuum level, printing height, temperature of the printhead and substrate etc. will be optimized according to achieve a reliable, high resolution printing. Scanning electron microscope (SEM), XRD (X-ray Diffraction) and Atomic force microscope (AFM) will be used to conduct material/chemical/surface analyses for each step of this new printing process.

1.3.2 Objective 2: Fabricate flexible copper patterns on polymer based substrate (PET)

We achieved objective 1 through efforts, functional copper patterns with high resolution and high conductivity were successfully fabricated on flexible photopaper substrate. But the photopaper substrate still has many limitations, for example it is easy to be torn, burn and corroded. What's more, we believe the relative rough surface of the photopaper limit the conductivity of deposited copper. So we decided to push the board of printed electronics forward and set our goal to make high conductivity copper patterns on PET substrate, a stable, smooth and transparent polymer based substrate.

While for the photopaper, it is relative easy to plant functional groups on its surface using a surface treatment method and this kind of surface treatment technique is mature in the industry. But for some other polymer based substrate such as PET/PI, the conventional wet chemical polyelectrolyte treatment process doesn't work well, since such substrate is chemically inert and you need to put lots of effort to make it active. What's more, conventional wet chemical surface treatment techniques create lots of chemical waste and

most of them is hazardous and harmful to human body. So we tried to propose another surface treatment process to form metallic circuits on hydrocarbon polymers using a unique hyperthermal hydrogen induced cross-linking (HHIC) technology to graft polyelectrolyte on polymers which is an environmental friendly, chemical-free method to achieve a strong adhesion between the deposited materials and the substrate. [39-42] After HHIC, the printed solution will bond together with the substrate, creating high conductivity copper patterns which have a very strong adhesion with the PET substrate after ELD process.

The proof-of-concept work was demonstrated in Chapter 3. The feasibility and merit of this printing process is that the grafted polyelectrolyte will act as an effective linker layer connecting the polymer substrate with the metal layer, resulting in a very strong adhesion between the deposited copper and the PET or PDMS substrate. The methodology will be also applied to other commercially available polymeric materials such as PC (polycarbonate), PE (Polyethylene), PVC (Polyvinyl chloride) and PI (Polyimide).

1.4 References

[1] J. Perelaer, P. J. Smith, D. Mager, D. Soltman, S. K. Volkman, V. Subramanian, *et al.*, "Printed electronics: the challenges involved in printing devices, interconnects, and contacts based on inorganic materials," *Journal of Materials Chemistry*, vol. 20, pp. 8446-8453, 2010.

[2] X. Wang, T. Li, J. Adams, and J. Yang, "Transparent, stretchable, carbon-nanotube-inlaid conductors enabled by standard replication technology for capacitive pressure, strain and touch sensors," *Journal of Materials Chemistry A*, vol. 1, pp. 3580-3586, 2013.

[3] X. Li, G. Wang, X. Wang, X. Li, and J. Ji, "Flexible supercapacitor based on MnO2 nanoparticles via electrospinning," *Journal of Materials Chemistry A*, vol. 1, pp. 10103-10106, 2013.

[4] D. Lupo, W. Clemens, S. Breitung, and K. Hecker, "OE-A Roadmap for Organic and Printed Electronics," in *Applications of Organic and Printed Electronics*, E. Cantatore, Ed., ed: Springer US, 2013, pp. 1-26.

[5] T. Sekitani and T. Someya, "Stretchable, Large-area Organic Electronics," *Advanced Materials*, vol. 22, pp. 2228-2246, May 25 2010.

[6] J. A. Rogers, T. Someya, and Y. G. Huang, "Materials and Mechanics for Stretchable Electronics," *Science*, vol. 327, pp. 1603-1607, Mar 26 2010.

[7] H. L. Filiatrault, G. C. Porteous, R. S. Carmichael, G. J. E. Davidson, and T. B. Carmichael, "Stretchable Light-Emitting Electrochemical Cells Using an Elastomeric Emissive Material," *Advanced Materials*, vol. 24, pp. 2673-2678, May 22 2012.

[8] A. E. Aliev, J. Y. Oh, M. E. Kozlov, A. A. Kuznetsov, S. L. Fang, A. F. Fonseca, *et al.*, "Giant-Stroke, Superelastic Carbon Nanotube Aerogel Muscles," *Science*, vol. 323, pp. 1575-1578, Mar 20 2009.

[9] D. H. Kim, N. S. Lu, R. Ma, Y. S. Kim, R. H. Kim, S. D. Wang, *et al.*, "Epidermal Electronics," *Science*, vol. 333, pp. 838-843, Aug 12 2011.

[10] F. Ding, H. Ji, Y. Chen, A. Herklotz, K. Dörr, Y. Mei, *et al.*, "Stretchable graphene: a close look at fundamental parameters through biaxial straining," *Nano letters*, vol. 10, pp. 3453-3458, 2010.

[11] X. Wang, H. Hu, Y. Shen, X. Zhou, and Z. Zheng, "Stretchable conductors with ultrahigh tensile strain and stable metallic conductance enabled by prestrained polyelectrolyte nanoplatforms," *Advanced Materials*, vol. 23, pp. 3090-3094, 2011.

[12] Y. Xia, B. Gates, Y. Yin, and Y. Lu, "Monodispersed colloidal spheres: old materials with new applications," *Advanced Materials,* vol. 12, pp. 693-713, 2000.

[13] K. Nomura, H. Ohta, A. Takagi, T. Kamiya, M. Hirano, and H. Hosono, "Room-temperature fabrication of transparent flexible thin-film transistors using amorphous oxide semiconductors," *Nature,* vol. 432, pp. 488-492, 2004.

[14] D. C. Hyun, M. Park, C. Park, B. Kim, Y. Xia, J. H. Hur, *et al.*, "Ordered zigzag stripes of polymer gel/metal nanoparticle composites for highly stretchable conductive electrodes," *Advanced Materials,* vol. 23, pp. 2946-2950, 2011.

[15] D. H. Kim and J. A. Rogers, "Stretchable electronics: Materials strategies and devices," *Advanced Materials,* vol. 20, pp. 4887-4892, 2008.

[16] Z. Yu, Q. Zhang, L. Li, Q. Chen, X. Niu, J. Liu, *et al.*, "Highly Flexible Silver Nanowire Electrodes for Shape‐Memory Polymer Light‐Emitting Diodes," *Advanced Materials,* vol. 23, pp. 664-668, 2011.

[17] Z. Zhang, C. Shao, P. Zou, P. Zhang, M. Zhang, J. Mu, *et al.*, "In situ assembly of well-dispersed gold nanoparticles on electrospun silica nanotubes for catalytic reduction of 4-nitrophenol," *Chem. Commun.*, vol. 47, pp. 3906-3908, 2011.

[18] Z. Liu, S. Tabakman, K. Welsher, and H. Dai, "Carbon nanotubes in biology and medicine: in vitro and in vivo detection, imaging and drug delivery," *Nano research,* vol. 2, pp. 85-120, 2009.

[19] K. S. Kim, Y. Zhao, H. Jang, S. Y. Lee, J. M. Kim, K. S. Kim, *et al.*, "Large-scale pattern growth of graphene films for stretchable transparent electrodes," *Nature,* vol. 457, pp. 706-710, 2009.

[20] T. Sekitani, Y. Noguchi, K. Hata, T. Fukushima, T. Aida, and T. Someya, "A rubberlike stretchable active matrix using elastic conductors," *Science,* vol. 321, pp. 1468-1472, 2008.

[21] Y. Zhang, C. J. Sheehan, J. Zhai, G. Zou, H. Luo, J. Xiong, *et al.*, "Polymer‐Embedded Carbon Nanotube Ribbons for Stretchable Conductors," *Advanced Materials,* vol. 22, pp. 3027-3031, 2010.

[22] S. Eichhorn, A. Dufresne, M. Aranguren, N. Marcovich, J. Capadona, S. Rowan, *et al.*, "Review: current international research into cellulose nanofibres and nanocomposites," *Journal of Materials Science,* vol. 45, pp. 1-33, 2010.

[23] D. Bloor, K. Donnelly, P. Hands, P. Laughlin, and D. Lussey, "A metal–polymer composite with unusual properties," *Journal of Physics D: Applied Physics,* vol. 38, p. 2851, 2005.

[24] J. Busfield, A. Thomas, and K. Yamaguchi, "Electrical and mechanical behavior of filled elastomers 2: The effect of swelling and temperature," *Journal of Polymer Science Part B: Polymer Physics,* vol. 42, pp. 2161-2167, 2004.

[25] D. J. Lipomi, M. Vosgueritchian, B. C. Tee, S. L. Hellstrom, J. A. Lee, C. H. Fox, *et al.*, "Skin-like pressure and strain sensors based on transparent elastic films of carbon nanotubes," *Nature nanotechnology,* vol. 6, pp. 788-792, 2011.

[26] G. Catalan and J. F. Scott, "Physics and applications of bismuth ferrite," *Advanced Materials,* vol. 21, pp. 2463-2485, 2009.

[27] D. Yoon, Y.-W. Son, and H. Cheong, "Strain-dependent splitting of the double-resonance Raman scattering band in graphene," *Physical Review Letters,* vol. 106, p. 155502, 2011.

[28] D. S. Germack, C. K. Chan, B. H. Hamadani, L. J. Richter, D. A. Fischer, D. J. Gundlach, *et al.*, "Substrate-dependent interface composition and charge transport in films for organic photovoltaics," *Applied Physics Letters,* vol. 94, p. 233303, 2009.

[29] A. Teichler, J. Perelaer, and U. S. Schubert, "Inkjet printing of organic electronics - comparison of deposition techniques and state-of-the-art developments," *Journal of Materials Chemistry C,* vol. 1, pp. 1910-1925, 2013.

[30] A. R. Uhl, C. Fella, A. Chirila, M. R. Kaelin, L. Karvonen, A. Weidenkaff, *et al.*, "Non-vacuum deposition of Cu(In,Ga)Se2 absorber layers from binder free, alcohol solutions," *Progress in Photovoltaics,* vol. 20, pp. 526-533, Aug 2012.

[31] S. Ito and Y. Mikami, "Porous carbon layers for counter electrodes in dye-sensitized solar cells: Recent advances and a new screen-printing method," *Pure and Applied Chemistry,* vol. 83, pp. 2089-2106, Aug 2011.

[32] R. Ramasubramaniam, J. Chen, and H. Liu, "Homogeneous carbon nanotube/polymer composites for electrical applications," *Applied Physics Letters,* vol. 83, p. 2928, 2003.

[33] J. G. Simmons, "Generalized formula for the electric tunnel effect between similar electrodes separated by a thin insulating film," *Journal of Applied Physics,* vol. 34, p. 1793, 1963.

[34] M. J. Joralemon, S. McRae, and T. Emrick, "PEGylated polymers for medicine: from conjugation to self-assembled systems," *Chemical Communications,* vol. 46, pp. 1377-1393, 2010.

[35] B. Straumal, A. Mazilkin, S. Protasova, A. Myatiev, P. Straumal, E. Goering, *et al.*, "Amorphous grain boundary layers in the ferromagnetic nanograined ZnO films," *Thin Solid Films,* vol. 520, pp. 1192-1194, 2011.

[36] S. A. Yousem, S. Dacic, Y. E. Nikiforov, and M. Nikiforova, "Pulmonary Langerhans Cell Histiocytosis," *CHEST*, vol. 143, pp. 1679-1684, 2013.

[37] S. Jeong, S. H. Lee, Y. Jo, S. S. Lee, Y.-H. Seo, B. W. Ahn, *et al.*, "Air-stable, surface-oxide free Cu nanoparticles for highly conductive Cu ink and their application to printed graphene transistors," *Journal of Materials Chemistry C*, vol. 1, pp. 2704-2710, 2013.

[38] H. H. Chen, R. Anbarasan, L. S. Kuo, M. Y. Tsai, P. H. Chen, and K. F. Chiang, "Synthesis, characterizations and hydrophobicity of micro/nano scaled heptadecafluorononanoic acid decorated copper nanoparticle," *Nano-Micro Letters*, vol. 2, pp. 101-105, May 2010.

[39] Y. Liu, D. Q. Yang, H. Y. Nie, W. M. Lau, and J. Yang, "Study of a hydrogen-bombardment process for molecular cross-linking within thin films," *Journal of Chemical Physics*, vol. 134, Feb 21 2011.

[40] Z. Zheng, W. M. Kwok, and W. M. Lau, "A new cross-linking route via the unusual collision kinematics of hyperthermal protons in unsaturated hydrocarbons: the case of poly(trans-isoprene)," *Chemical Communications*, pp. 3122-3124, 2006.

[41] Z. Zheng, X. D. Xu, X. L. Fan, W. M. Lau, and R. W. M. Kwok, "Ultrathin polymer film formation by collision-induced cross-linking of adsorbed organic molecules with hyperthermal protons," *Journal of the American Chemical Society*, vol. 126, pp. 12336-12342, Oct 6 2004.

[42] D. B. Thompson, T. Trebicky, P. Crewdson, M. J. McEachran, G. Stojcevic, G. Arsenault, *et al.*, "Functional Polymer Laminates from Hyperthermal Hydrogen Induced Cross-Linking," *Langmuir*, vol. 27, pp. 14820-14827, Dec 20 2011.

Chapter 2

2 Fabrication of flexible high resolution copper patterns on photopaper

Almost all the printed electronics fabrication techniques are based on directly inkjet printing nanoparticle. As we mentioned in chapter 1, high cost (silver nanoparticle is expensive), low conductivity and unreliable printing (nozzle often got clogged because of the accumulation of nanoparticle) are three critical issues for today's printed electronics fabricating industry. What we tried to achieve in this project was reducing the cost, enabling reliable high resolution printing and creating copper patterns with high conductivity. So in this chapter, a new method of fabricating copper circuits on flexible photopaper with high resolution and high conductivity will be demonstrated, solving all the problems mentions above.

2.1 Introduction

Printed flexible electronics and devices which can maintain functionality when subject to a large deformation and stress are highly desirable in nowadays high-tech industry and daily life. Conventional electronic fabrication systems are mostly based on photolithography, a complex and time-consuming process that involves large volumes of hazardous waste and expensive facilities. [1] The emerging nanotechnology is also evolved in fabricating electronics such as solar cell and super capacitor, however, its high cost and requirement for high-end facilities limit its appeal. [2] There is increasing demand for high quality and low cost electronic components such as RFID tags, supercapacitor, flexible sensor and devices, which require innovative fabrication techniques that are faster but cheaper compared to traditional production methods. [3-5]

It is predicted that the market of flexible organic and printed electronics will exceed $300 billion by 2028. [6] In this regard, techniques such as inkjet printing, [7] non-vacuum deposition [8] and screen printing [9] have emerged as promising technical trends to produce flexible electronics and devices. Among these, inkjet printing technology has gained more and more attention in recent years for its appeal of low-cost, non-contact, low material consumption, maskless and additive printing procedure.

Inkjet printing, which is widely used in home and office, has also been employed extensively as a low cost tool to explore various aspects of printed electronics in a laboratory setting, [10, 11] such as ITO free polymer solar cell, functional polymer films, [12] complex heterogeneous tissue constructs [13] and thin film transistors. [14] Applied to printed electronics based on inkjet printing, most of the research efforts are focused on direct printing of metal nanoparticles or conductive polymer, followed by sintering to make them conductive. Cu- or Ag-nanoparticle based inks were commonly printed on a treated PET/PI substrate, with a nozzle size of larger than 10 μm, and dimension of the final resulted metal pattern is normally around 10-20 μm, five times better than the current resolution of screen printing. However, clogging is always a common critical issue for micron size nozzles due to the accumulation of nanoparticles at the nozzle opening. Other critical issues reside in the oxidization and sedimentation stability of the corresponding inks, generally requiring large amounts of stabling and decoration agent and is in a very low concentration of metal particles [15, 16] which consequently leads to a high resistance of the printed patterns. So in our method, we choose to print pure catalyst noble-metal-containing salt solution to overcome the issue of nozzle blocking and enables greater printing resolution.

In this project, we have developed a convenient, ultra-low-cost method of inkjet printing combined with electroless deposition (ELD) process to prepare high-resolution metal patterns. [17-20] ELD is an auto-catalytic technique used to deposit metals (copper, nickel, etc.) on various substrate such as paper, plastic, aluminum oxide, and even yarns. [21-23] The mechanism of ELD was thoroughly studied these years, making it a convincing technique for making metal coating and high resolution patterns. [24] Abundant metal ions in the ELD bath can create patterns with dense surface, which in turn results in good conductivity close to bulk metals. This absolute advantage drives us to involve this technique in the fabrication of flexible electronics.

Fig. 1 schematically shows the entire process of our method, which typically includes three steps, inkjet printing noble-metal-containing salt solution onto polyelectrolytes modified substrate, ELD of copper and thermal sintering. Loading of noble-metal moieties onto substrates involved a typical chemistry reaction of ion exchange, i.e., the noble-metal moieties like $PdCl_4^{2-}$ take places of anions of Br- because of their higher affinity to quaternary ammonium in the chain of polyelectrolytes. [25] As a proof-of-concept, $(NH_4)_2PdCl_4$ and Epson photopaper with polyelectrolytes modification were chosen to demonstrate the process. Influence of printing parameters was thoroughly studied and the optimum parameters such as jetting voltage control waveform, drop space, jetting frequency and meniscus vacuum were obtained. As a result, functional copper patterns with conductivity up to 3.9×10^7 S/m (65% of bulk copper) and a feature dimension down to 50 μm were successfully fabricated. No extreme condition was needed and all processing steps were conducted under regular laboratory conditions.

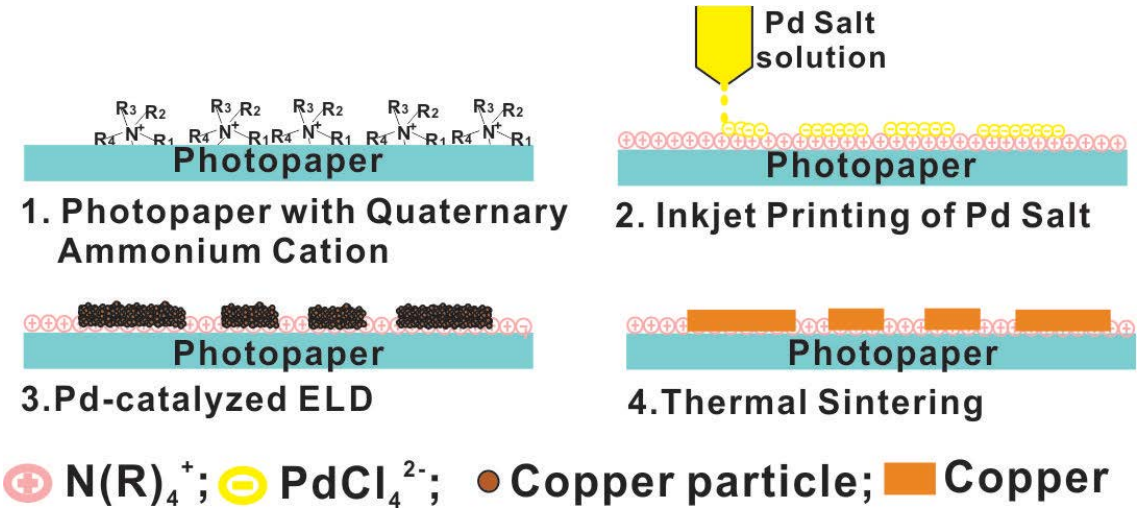

Figure 1: Schematic illustration of paper-based metal patterns with high resolution and conductivity via printing catalyst and subsequent ELD process.

2.2 Theory

2.2.1 Inkjet printing

Inkjet printing is a kind of technology that used for creating patterns or images by propelling ink droplets onto different substrate, such as paper, photopaper, PET, PI, PDMS films, etc. The idea of inkjet printing is very old and originated in the 19th century, but was not commercialized at that time. Till 1970s, with the development of computer and digital image technology, inkjet printer started gaining their market. Companies such as Epson, HP, Xerox and Lexmark rose up by making inkjet printer for office use. Several technical revolution has taken place during the past 20 year and right now there are two main streams of printing technologies used in contemporary inkjet printer, one is call continuous printing (CIJ) and the other is called Drop-on-demand printing (DOD).

The principle of continuous inkjet printer is shown in Fig. 2. [26] Printing ink is pressurized by a pump (the ink supply pump) and flow from the cartridge to the nozzles.

Very small ink droplets are then jetted through the nozzle at high speed. The ejected droplets then pass through a pair of charge electrode and are selectively charged according to the printed image data. Charged droplets then pass through a pair of deflection electrode where a high voltage is applied and are separated according to their charge. After that, the charged droplets hit the substrate from bottom to top. Either the substrate plate or the printing nozzle can move in X and Y directions, creating a two-dimensional pattern with dot matrix on the substrate. Non-charged droplets will flow straight to the gutter and then return as ink to the ink cartridge. Inkjet printer based on this principle is losing its popularity these years, since it is expensive, hard to maintain and need high level operative skills --- you need to adjust the orifice-shape and fix the orifice in place manually sometimes.

For the drop-on-demand inkjet printing technology, printers only eject droplets of ink when they are required by the system. So a deflection system with high voltage or ink recycling system is no longer needed. Fig. 3 shows the principle of a drop-on-demand inkjet printhead. One of the key component on the printhead is the jetting control system which can be divided into two kinds, the thermal inkjet and the piezoelectric inkjet. The thermal DOD inkjet printing utilizes a heating component inside the print head used for vaporizing some of the ink and creating a micro bubble. The formation of the bubble which increase its volume by heating forces a drop of ink out the nozzle, realizing the inkjet printing. While for the piezoelectric printhead, a piezoelectric membrane (reservoir) is placed upon a small ink chamber, the deformation of the piezoelectric membrane under different voltage will them force a drop of ink out the nozzle. By

controlling the jetting voltage value and jetting voltage waveform, the size of the droplets can be precisely controlled, enabling a robust high resolution printing.

.

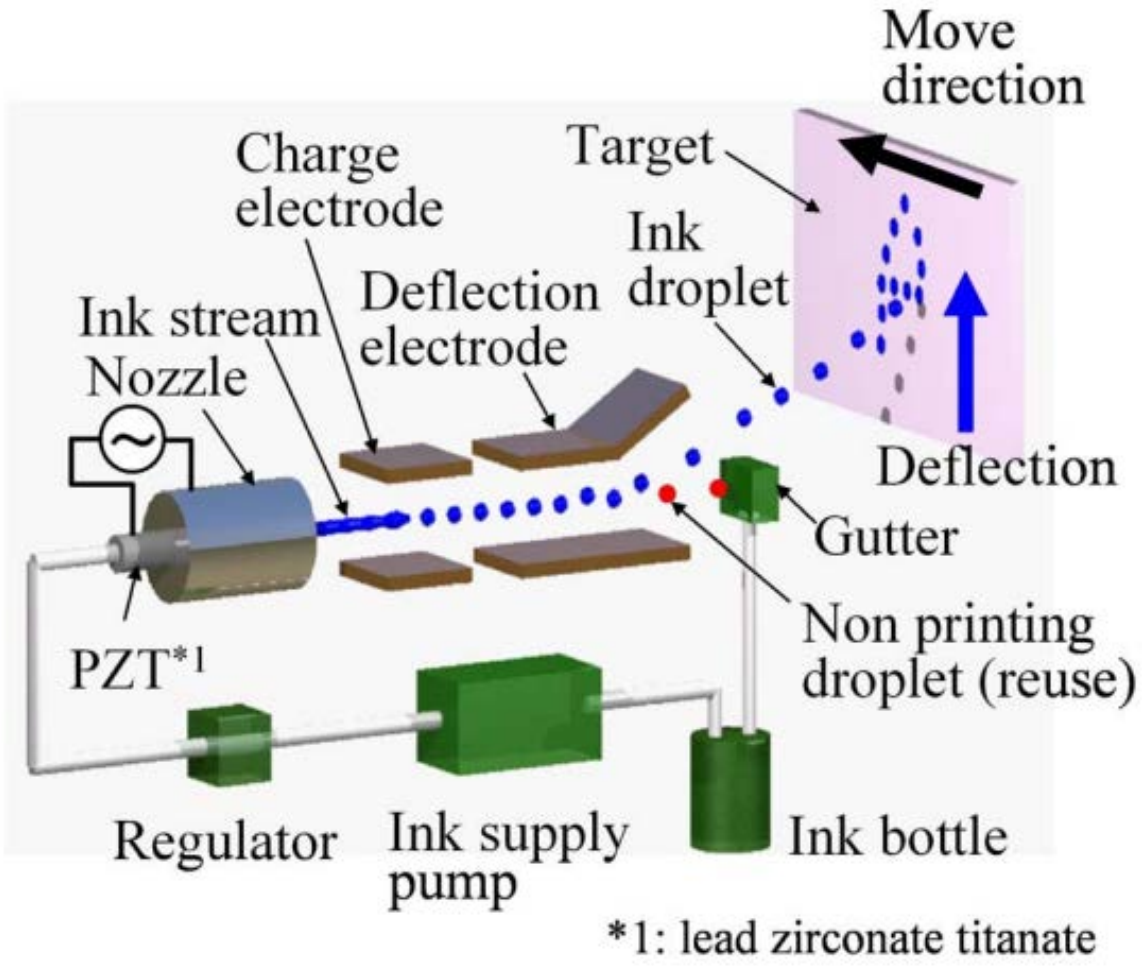

Figure 2: Principle of continuous inkjet printer. (Copy from [26])

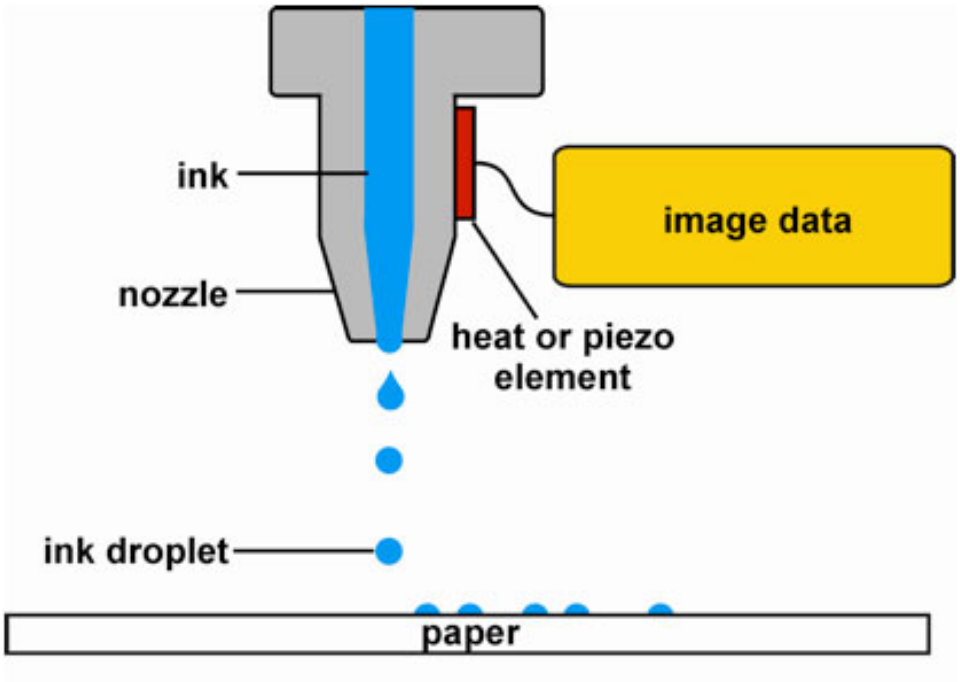

Figure 3: Principle of drop-on-demand inkjet printer. (Copy from [10])

Regarding all these pros and cons, we finally chose a DOD inkjet printer as our printing tool, for its ability of room temperature jetting, relative low cost and controllable jetting waveform. The model we used in this project is Dimatix DMP-2800 DOD materials printer, shown in Fig.4.

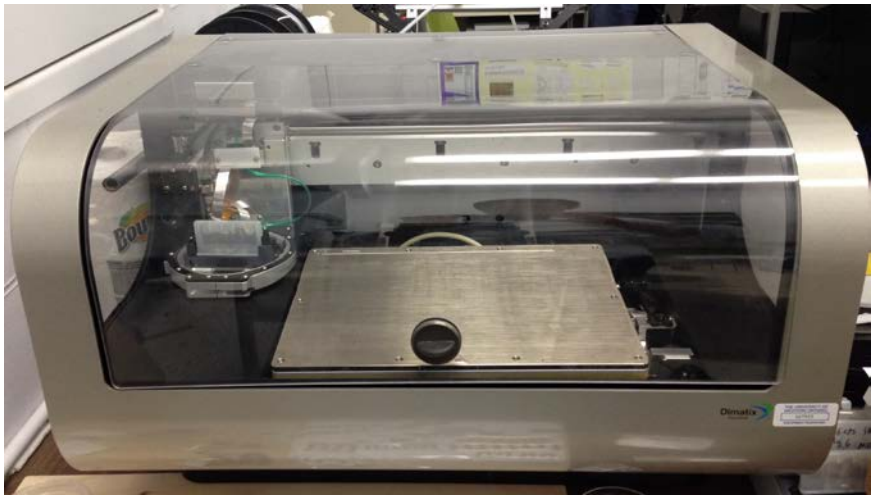

Figure 4: Dimatix DMP-2800 DOD inkjet printer used for this project.

2.2.2 Electroless deposition

Electroless deposition or electroless plating is an auto-catalytic chemical reaction used for depositing a layer of metal, usually copper and nickel, on a solid substrate such as metal or plastic. It is the most important process for through hole plating (THP) of printed circuit boards (PCBs) using the indirect-conventional method. The most important benefit of this technique is that it is not necessary to apply an electric filed/current through the solution to make the reaction occur and in most cases the electroless deposition can form a well deposited metal film on the substrate under room temperature. Electroless copper deposition was first reported by Narcus [27] and more than ten years later this technique was commercialized. [28, 29] In recent years modified formulations have rapidly developed enabling a higher plating rate, higher plating quality and extremely stable conditions under a wide range of plating conditions. [30-32]

2.3 Materials and experiments set-up

2.3.1 Materials

The substrate used for printing was EPSON Ultra Premium Photopaper Glossy, treated with polyelectrolytes containing quaternary ammonium by Epson Company. Ammonium tetrachloropalladate (II) ($(NH4)_2PdCl_4$, 97%) and anhydrous glycerol ($C_3H_5(OH)_3$, 99%) used for ink preparation were bought from SIGMA-ALDRICH and AMRESCO respectively. Chemicals used for ELD process were copper (II) sulfate pentahydrate ($CuSO_4 \cdot 5H_2O$, 98%, SIGMA-ALDRICH), potassium sodium tartrate tetrahydrate ($C_4H_4KNaO_6.4H_2O$, 99%, SIGMA-ALDRICH), formaldehyde solution (HCHO, 36.5-38% in H_2O, SIGMA-ALDRICH) and Sodium Hydroxide (NaOH, 97%, CALEDON).

2.3.2 Preparation of the palladium salt ink

A glycerol-water solution with viscosity of ~11 centipoise (cp) was achieved by mixing anhydrous glycerol and distilled water in the ratio 3:2 by volume. [33, 34] Ammonium tetrachloropalladate (II) was then added, followed by four minutes mixing in the VWR mixer (Fig.5) until a clear dark yellow solution was obtained. The optimum viscosity for inkjetable fluids in piezoelectric Drop-on-Demand (DOD) printhead reported in literature is 10-12 cp at room temperature. [35] Based on these, inkjet printable inks containing different concentration of palladium ions were prepared and viscosity was measured. To find the optimum ink for the following inkjet printing and ELD process, solutions with different Pd salt concentration (10-60 mM) were prepared in the same way. All prepared inks were degassed under a vacuum chamber of 2 psi for 1 hour to remove dissolved gas, followed by filtering with a 0.2 μm springe filter to get rid of undesired particles which inhibits jetting. The final viscosity was measured with a Gilmont GV-2100 (Fig.6) Falling Ball Viscometer to further confirm it was in a proper range.

Figure 5: VWR mixer

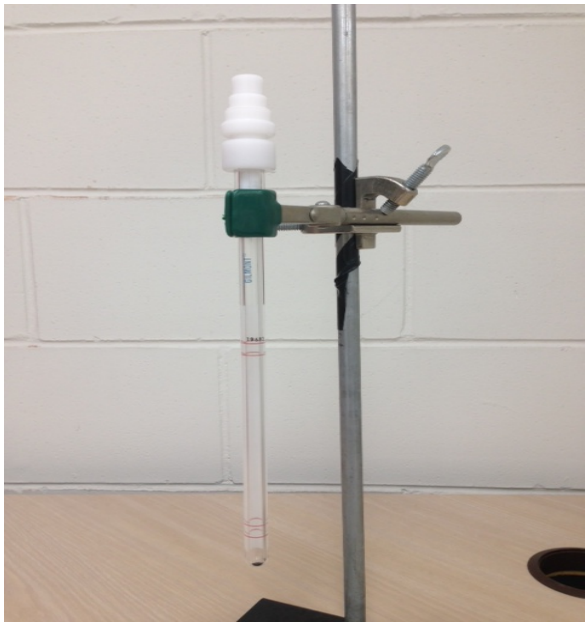

Figure 6: Gilmont GV-2100

2.3.3 Inkjet printing and parameters optimization

Printing patterns were designed and drew with vector drawing software with colour values set to R=0, G=0, B=0 and exported as binary bmp format in bitmap colour model with a resolution of 1300 ppi. Inkjet printing was performed using a commercially available inkjet Dimatix DMP-2800 materials printer (FUJIFIL Dimatix, USA, Fig.4), equipped with a 1 PL piezoelectric DOD 16-jet cartridge that can deposit features as small as 20 μm. Two cameras were installed in the printer, the high speed side view camera was used for monitoring the droplets in real time and the top view camera was for checking the printed patterns and move the print head to the position where you want to start the printing. The stage is an X-Y two directions vacuum stage with small hole-arrays on it, enabling a vacuum absorption between the substrate and stage. Inkjet printing experiment set up is shown in Fig.7.

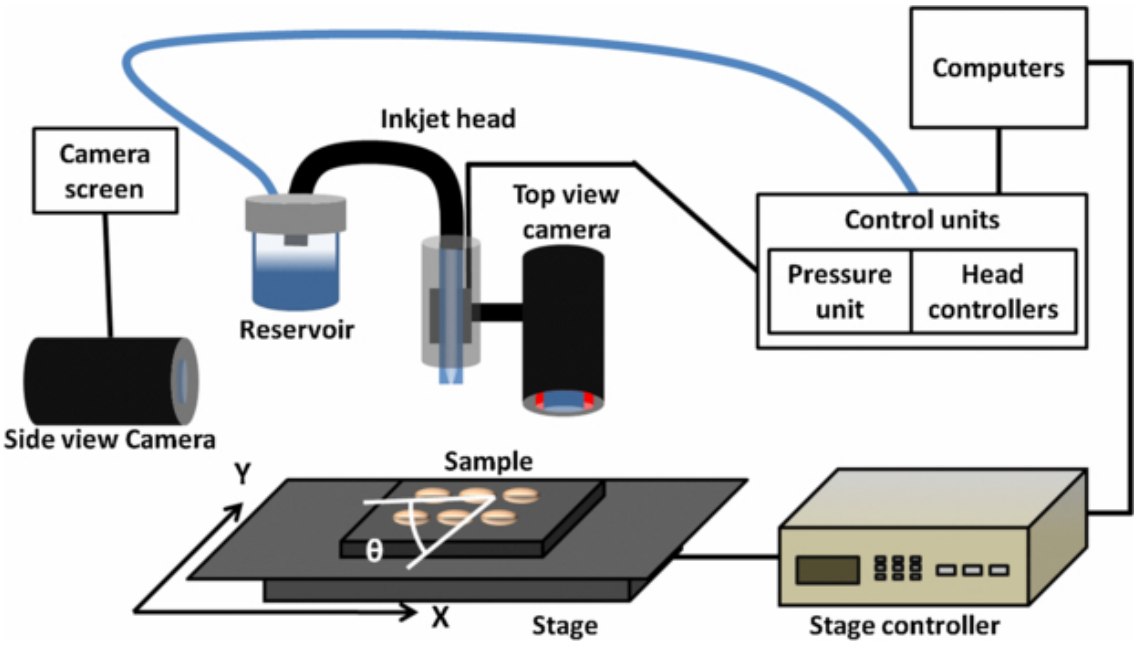

Figure 7: Inner structure of the inkjet printing system (Copy from [36])

Printing parameters such as jetting period, jetting voltage control waveform, meniscus vacuum, printhead temperature were dynamically adjusted according to the real-time droplets video generated by a built-in high frequency camera (side view camera in Fig.7). Epson Ultra-Premium Glossy photopaper was used as the substrate for printing and was cut into a 10 cm x 10 cm square to reduce deformation caused by heating and wetting. Prepared photopaper was placed on a vac-sorb substrate with temperature at 30°C and fixed by scotch tape. Lines of the same width were printed with the drop space set to 20 µm, 25 µm, 30 µm and 35 µm respectively and examined by microscope. Results showed a drop space of 25 µm giving the best pattern thus complex and functional patterns were then printed with optimum settings (maximum jetting frequency 20 kHz, drop space 25 µm, meniscus vacuum 3.5 H_2O, printhead temperature 30°C, printhead angle 3.6°, jetting period 41.792 µs, jetting voltage 23.60 ± 0.4 V, printing height 150 µm, cleaning cycle of 1 s purging –1 s spitting –2 s blotting, tickle mode on with frequency 2 kHz).

2.3.4 ELD of copper and thermal sintering

ELD process was conducted to apply copper pattern onto the printed feature. The detailed process of ELD can be found in former literatures. [18, 37, 38] Briefly, patterns printed with inks featuring Pd salt concentration of 10 mM, 20 mM, 30 mM, 35 mM, 40 mM, 45 mM, 50 mM, 55 mM and 60 mM were put into a plating bath containing 1:1 mixture of freshly prepared solutions I and II. Solution I consists of 13 g/L $CuSO_4 \cdot 5H_2O$, 12 g/L NaOH and 29 g/L $KNaC_4H_4O_6 \cdot 4H_2O$ which were added into distilled water in sequence. Solution II is 9.5 mL/L HCHO in distilled water. Deposition time was controlled to 30 min, 40 min, 60 min, 120 min, and 180 min for printed patterns under the same setting. Deposited copper lines were air dried and then put into a Fisher 1500 DEG Tube Furnace (Fig.8) for sintering. Nitrogen was flowing for 30 minutes before heating to ensure that no residual oxygen was in that tube. Sintering was kept for an hour under continuous nitrogen flow at 200°C and heating rate set to 15^{o}C/min. [39, 40]

Figure 7: Fisher 1500 DEG Tube Furnace

2.3.5 Characterization

The viscosity of the inks was measured by a Gilmont GV-2100 Falling Ball Viscometer using a 316 stainless steel (SS) high-precision ball with a 7 mL of sample volume. Real time images of the droplets were captured with a CORRECT PL- 4x40 built-in camera. For studying the surface of electroless plated copper patterns before and after sintering, a GENTAUR NJF-120A metallurgical microscope and a NOVEL Optics HDCE-90D (3488X2616) CCD camera were used to obtain the image of the pattern. A Hitachi S-4500 field emission scanning electron microscopy (SEM) was also used to observe the surface morphologies of the plated patterns. Atomic force microscope (AFM, Dimension V equipped with a Nanoscope controller V and Nanoscope software 7.30, Veeco) was used to obtain height information. Chemical composition information of the samples was obtained with a Kratos Axis Ultra spectrometer using a monochromatic A1 Kα radiation source. Adhesion was determined by the use of a cross scotch tape test, following ASTM D-3359 using 3M # 600 tape. [41] A four-probe method using M 2400 Keithley Multimeter was carried out to measure the sheet resistance, from which conductivity was calculated. X-ray diffraction analysis was done using Rigaku Ultima-IV XRD goniometer.

2.4 Results and discussion

2.4.1 Ink viscosity and stability

Negatively charged tetrachloropalladate group (-$PdCl_4^{2-}$) tends to form chemical bonds with the positively charged quaternary amine group (NR_4^+-) on the photopaper. A bivalent tetrachloropalladate group will combine with two monovalent quaternary amine groups when the ink droplet is in contact with the photopaper substrate which results in a

strong adhesion between the palladium ions and the substrate. Rate of ELD of copper as well as the plated copper density are proportional to the concentration of catalyst (palladium ion in this case), thus a high concentration of the palladium salt is preferred. [42, 43] However, the number of quaternary amine groups on the surface of photopaper is limited, which means excessive palladium salt will result in unbonded palladium ions on the surface. Unbonded ions will disperse on the photopaper and dissolve in deposition solution during the process of ELD, causing serious losses in resolution (compared experimental results are showed in Section 2.4.3-ELD of Copper). Therefore, inks with concentrations ranging from 10 mM to 60 mM were prepared to find the optimal solution.

Fig.8 shows that viscosity increases proportionally with concentration of ammonium tetrachloropalladate. Yet, all prepared inks were still in the range of the optimum requirement (10 ~ 12 cp) for printing. In order to investigate the stability of the $(NH_4)_2PdCl_4$ ink, four tubes of prepared solution (45 mM) were store in a constant 4°C refrigerator and another four tubes (also 45 mM) were stored in a dark cabinet at room temperature (22°C). Colour change of the inks was checked daily. UV/Vis spectrometer measurements were taken to characterize the status of the inks and the results are shown in Fig. 9. For inks stored at room temperature, visible precipitation was clearly observed three days later and gradually increased with time. In order to rule out any effects of the sediment and get a reasonable result, we filtered the ink with a 0.2 μm syringe filer each time before the UV/Vis measurements (Fig. 9).

To get rid of the influence of the light on the stability of the inks, all prepared inks were stored in dark. Both the fresh inks and the samples stored at 4 °C for 180 days exhibited

an absorption peak at ~390 nm originating from two transitions of the $PdCl_4^{2-}$. [44] One day later at room temperature, the maximum absorption peak of the solution had shifted to ~375 nm and the absorptivity was also lightly reduced, indicating the decrement of the $PdCl_4^{2-}$ concentration and hydration to $PdCl_2(H_2O)_2$ and $[PdCl(H_2O)_3]^+$. Spectra of inks after three days showed an absorption peak at ~250 nm and a slight shift back to longer wavelengths in lower absorption values as time increased, attributing to the formation of $[Pd(H_2O)_4]^{2+}$ and reduced palladium ion. The decrement of the palladium ion concentration and the increasingly forming precipitation is probably due to the self-oxidation-reduction reaction of the Pd ion aquo-complex which results in the increment of relative chloride concentration, leading to the formation of $[PdCl(H_2O)_3]^+$ and $PdCl_2(H_2O)_2$. The palladium salt solutions after standing up to 180 days at 4°C showed no precipitation or deterioration. The colour of the ink is still dark yellow just as that of the initial solution. The ink remained stable under 4°C for more than 180 days without observation of sediment and also showed its capability of producing successful printing results. Inks stored under room temperature after 30 days still showed its ability to trigger the ELD process, but the ELD process was in a very low rate, usually taking more than three hours to complete and the deposited patterns were no longer uniform and continuous, indicating that such inks were no longer suitable for making a high resolution functional circuits. Thus, all the inks used for final printing were either fresh made or those stored at 4°C.

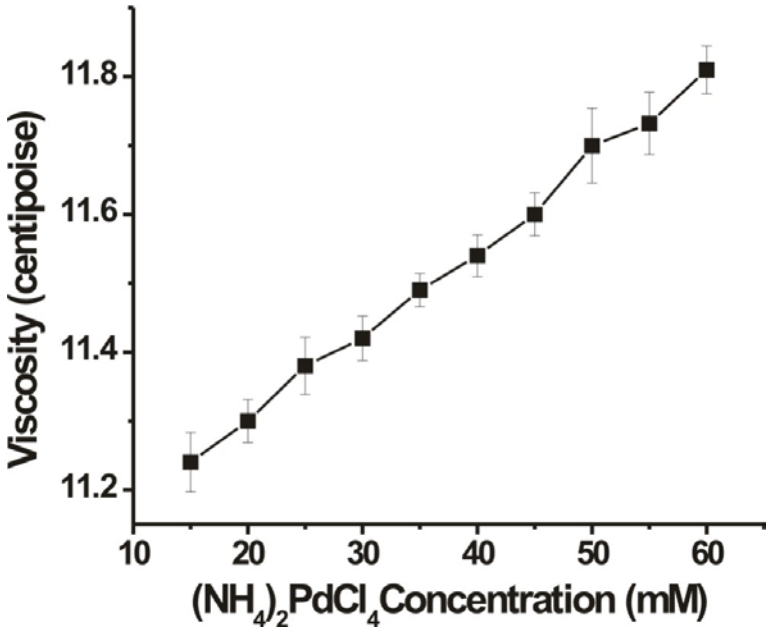

Figure 8: Viscosity of inks with different Pd salt concentration

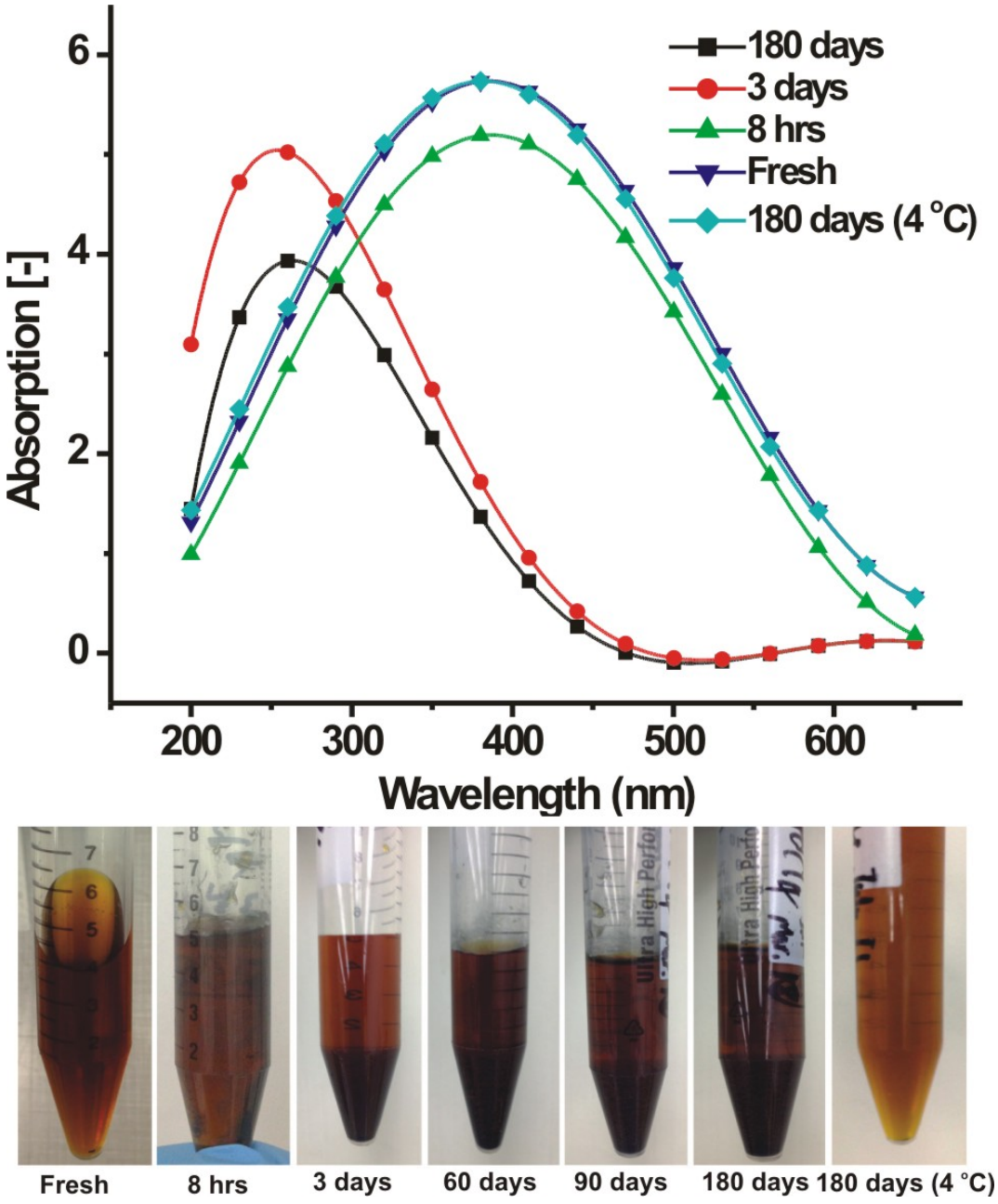

Figure 9: UV/visible-spectra (fitted) results of freshly prepared palladium (II) salt ink (triangle facing down) and inks after storage at room temperature for 8 hours (triangle facing up), 3 days (round circle), 180 days (square) and 180 days stored under 4 °C (diamond)

2.4.2 Inkjet printing of salt solution

The cartridge of ink jetting devices is always operated under negative pressure to keep the meniscus at the edge of the nozzle and prevent the ink from dripping under the action of gravity. The pressure difference between the inside and outside of the cartridge, which is also known as the meniscus vacuum, needs to be adjusted depending on the viscosity and surface tension of the ink. To obtain the optimum meniscus vacuum level, a built-in camera was used to monitor the formation of droplets in real time. Meniscus vacuum level was set to 3.2, 3.3, 3.5, 3.8 and 4.0 (inches of water) and under each level the printhead continuously worked for ten minutes. Results showed that a meniscus vacuum of 3.5 H_2O gave the most stable and reliable ejected droplets. Leakage was observed on some of the nozzles when the vacuum level was lower than 3.5 H_2O. Sate of the ink droplets under different jetting parameters is shown in Fig.10 ((a) Misdirected jetting caused by accumulated leaked ink around the nozzle. (b) Satellite droplets caused by relative high jetting voltage. (c) Droplets after applying the optimum parameters (meniscus vacuum: 3.5 H_2O, jetting voltage peak ~24.30 V, single jetting duration: 32.192 µs (phase 1: 9.792 µs, phase 2: 6.160 µs, phase 3: 8.496 µs, phase 4: 5.184 µs), maximum jetting frequency: 20 kHz)) The leaked ink attached and accumulated around the nozzle, causing misdirected jetting and blocked nozzle Fig. 10a. For the vacuum level higher than 3.5 H_2O, a relative high voltage (~28 V) must be applied to the nozzle in order to overcome the excessive negative pressure to make it jet. However, the increased voltage results in the breakup of the liquid ligament and large deformation of the piezo membrane which consequently leads to the generation of a primary drop and one or several satellite droplets (Fig. 10b). [21] Typically, the satellite droplets may cause

undesired patterns and a serious loss in resolution, and therefore should be avoided as much as possible. For the piezoelectric printhead, the velocity of droplet ejected from the nozzle is a function of applied peak voltage. We observed that the distance (from the nozzle plate to the place where droplet fully formed) travelled by the droplet also increased with the applied voltage. Higher voltage results in a bigger dot diameter because of the increased ink droplet's mass and velocity, which means a reduction in the printed resolution. By applying a meniscus vacuum of 3.5 H_2O, the optimum jetting voltage peak for the palladium ink was found to be ~24.3 V using the same real-time monitoring method. Fig. 10c shows the images of the perfect droplets ejected from the nozzle after applying the optimum parameters.

Nozzle clog was observed sometimes during real-time monitor, which was unacceptable for a high resolution printing. Since all the inks were degased and filtered by a 0.2 μm syringe filter, clogging should not be caused by undesired large particles or bubbles in the ink. Thus, the great possibility may reside in the voltage waveform used for controlling the bimorph on each nozzle. The bimorph is slightly deflected so that the fluid chamber above the nozzle is depressed by a bias voltage. Typically, the voltage waveform is divided into four segments, and each segment has three properties: slew rate, duration and level. [45] The first segment is called the loading work during which a decreased voltage is applied to the bimorph at the beginning of the jetting, bringing the bimorph back to a relaxed position with the chamber at its maximum volume. However, for the palladium salt ink the loading work segment will lead to the generation of micro-bubbles in the nozzle, prohibiting formation of droplets since the nozzle works in a high jetting frequency up to 20 kHz. Effect of such micro-bubbles is magnified in a nozzle with a

diameter of only 10 micron. Thus, we reduced the decreased level of the first phase, and got the optimum jetting waveform shown in Fig. 11. A reduced level (~ 50% of the initial one) of jetting voltage was applied to phase one, so as a longer duration of 2.550 μs, to prevent the generation of micro-bubbles. A dampening segment was applied to phase four to prevent the nozzles from sucking air back in and get prepared for the next ejection. A video of the nozzles' jetting with the optimum jetting waveform, meniscus vacuum value (3.5 H_2O) and jetting voltage peak (~ 24.30 V) was take, showing a well alignment, stable jetting (please refer to the support information). No clog or misdirected jetting occurred during continuous working for one hour, revealing a robust and high-resolution printing with ammonium tetrachloropalladate (II) solution was achieved.

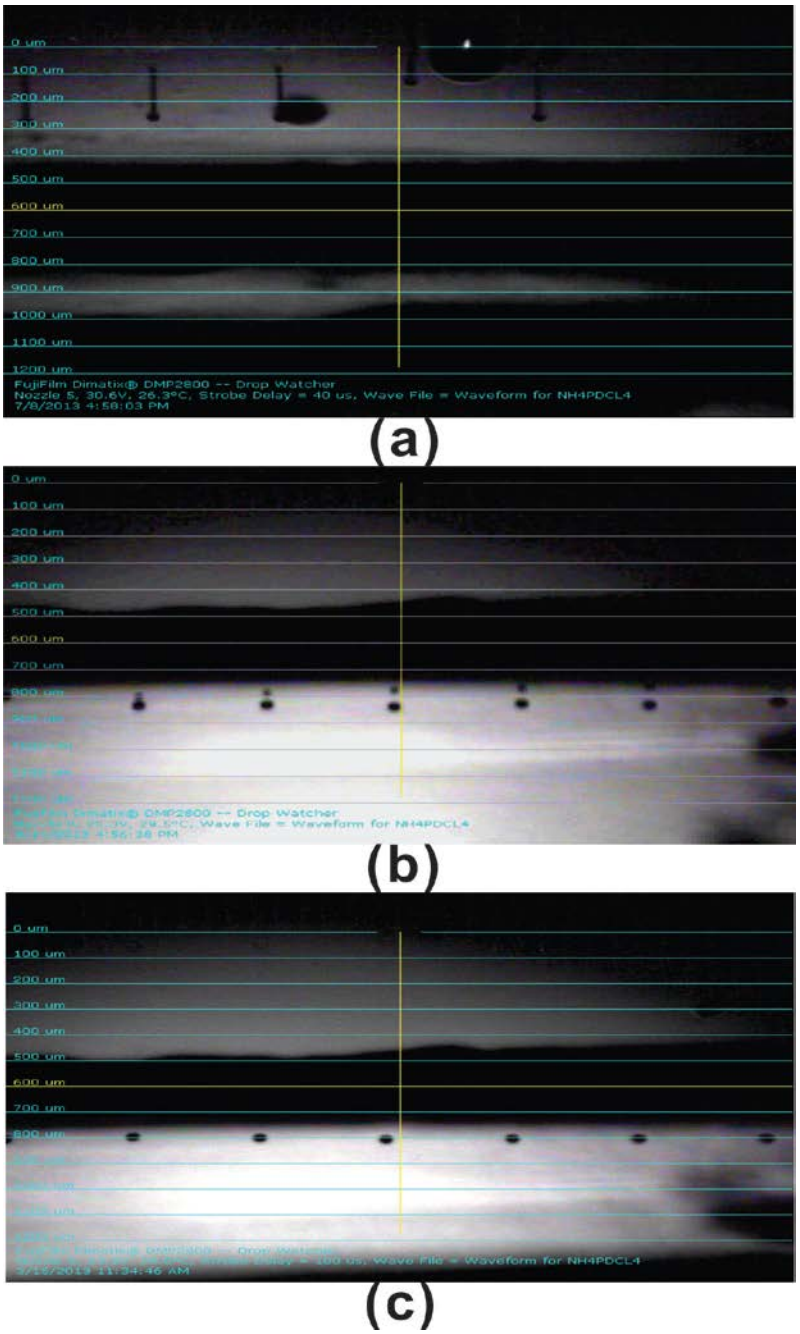

Figure 10: Droplets pictures under different jetting conditions (a) Misdirected jetting caused by accumulated leaked ink around the nozzle. (b) Satellite droplets caused by relative high jetting voltage. (c) Droplets after applying the optimum parameters (meniscus vacuum: 3.5 H2O, jetting voltage peak ~24.30 V, single jetting duration: 32.192 µs (phase 1: 9.792 µs, phase 2: 6.160 µs, phase 3: 8.496 µs, phase 4: 5.184 µs), maximum jetting frequency: 20 kHz).

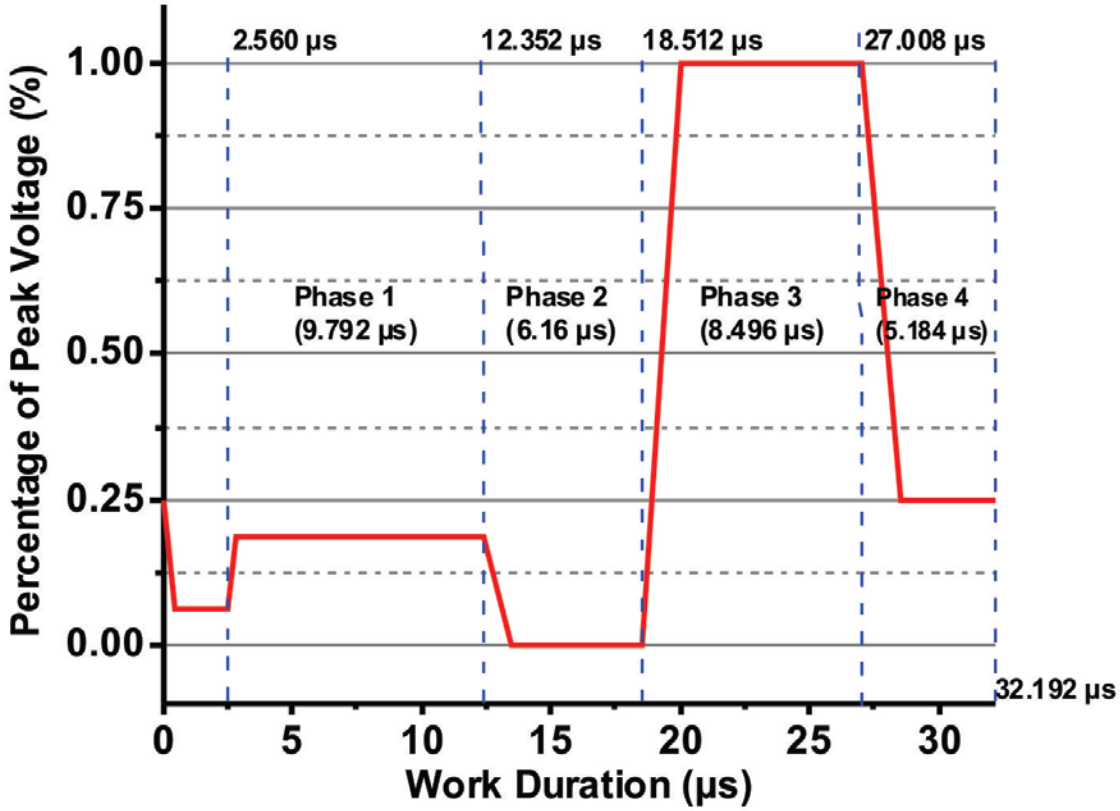

Figure 11: Modified waveform for the ammonium tetrachloropalladate (II) ink

2.4.3 ELD and conductivity

ELD of copper was conducted under ambient environment, showing a satisfied deposition rate. Table 1 shows the deposition results of patterns printed with inks of different concentration. Patterns used for testing were 3 mm x 3 mm squares, printed under the same condition with inks at different concentration.

Table 1: ELD of copper results of patterns printed with different concentration (Scale bar: 1 cm)

Sample No.	PdCl42- Concentration	Time	Results
1	10 mM	3 hours	No copper
2	20 mM	3 hours	No copper
·3	30 mM	2 hours	
4	35 mM	2 hours	
5	40 mM	1 hour	
6	45 mM	40 mins	
7	50 mM	40 mins	
8	55 mM	30 mins	
9	60 mM	30 mins	

Patterns were taken out of the deposition solution when no observable changes happened to their surfaces. Deposition time is 3~4 times longer than conventional ELD which usually happens on a PET or PI substrate. This may result from a smaller surface area of the reactive ions and a less active catalyst newly formed on the photopaper. The colour of the photopaper substrate after ELD process changed in different degrees, the longer the ELD process, the greater the colour changed. Two hours ELD made the colour of group #3, #4 changed from white to a little bit green, while for group #5 - #9 which the time of ELD process was controlled down to less than one hour, the photopaper still kept its white colour but became a little bit grey. No crack or damage was observed on the substrate of all ELD process time. Table 1 group #1 and #2 show that a concentration below 20 mM is not able to trigger the deposition, a relative long deposition time is

needed for patterns printed with ink concentration of ~30 - ~35 mM and copper plating will stop at a certain level of deposition resulting in an incomplete pattern. The half-stopping deposition is caused by the reduced copper activity as time goes on. Palladium ions first initiate the copper reduction, the reduced copper then serves as catalysts to keep the reaction going. The deposition rate need to be kept in a certain level so that the freshly reduced copper can maintain its activity and continue its serving as catalyst. A slow deposition rate caused by the ink of low concentration leads to loss of the activity of the reduced copper, which gives explanation to the incomplete pattern of group #3 and #4. Serious dispersion was observed when the ink concentration was above 50 mM (Table.1 group #7, #8, #9) since the limited number of quaternary amine on the photopaper couldn't form chemical bonds with the excessive amount of palladium salt. The unbonded palladium salt will then disperse in the photopaper and dissolve in the deposition solution, causing serious loss of resolution. The optimum concentration range was found to be around 40-45 mM and the dimension of the resulted copper patterns printed in this concentration were measured by an optical microscope, showing a slight increment in its width and length (~ 0.15 mm, ~4.5%) due to ink dispersion along the photopaper fibres. The ink with a concentration of 45 mM palladium salt was then adopted for the following complex and functional patterns printing.

Our former work reveals that the thickness of the plated copper is also a function of deposition time, but the increment of thickness is not unlimited. [18, 20] The maximum thickness varies depending on the catalyst concentration, type of substrate and catalyst. Because of the fibre properties of photopaper, most of the $PdCl_4^{2-}$ infiltrated into the substrate with solvent, some of them remained on the surface and bonded with the

quaternary amine groups along the paper fibre. Thus the amount of effective catalyst ($PdCl_4^{2-}$-) for the following ELD process is actually small, making the copper deposition rate relatively slow. Newly reduced copper loses its activity quickly and because of the slow rate, the amount of active copper quickly decreases making this auto-catalyst reaction stop. For the patterns printed with a 45 mM concentration of palladium salt on the photopaper, the copper will stop growing when its thickness reaches ~350 nm. The SEM image of the plated copper layer after a three hours ELD is showed in Fig. 12, showing the maximum thickness of the copper layer.

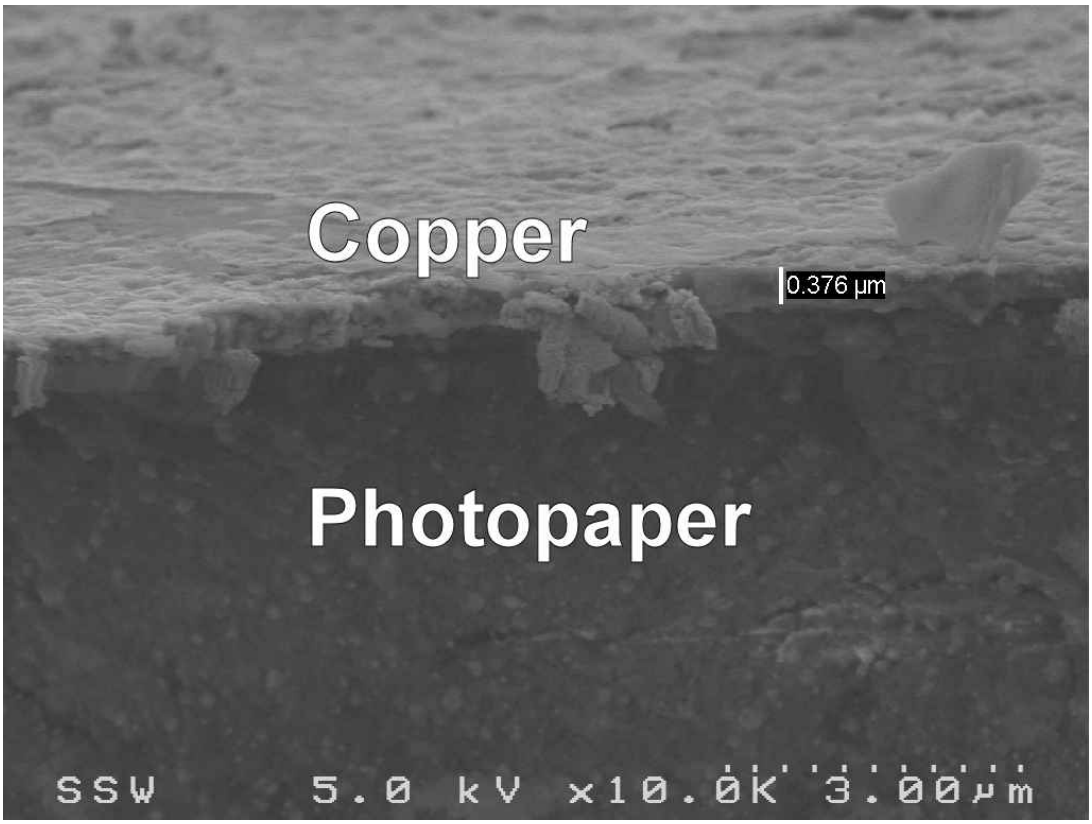

Figure 12: SEM image of the cross section of the ELD copper layer on photopaper

We adopted the present method for manufacturing flexible integrated circuits and the results are shown in Fig. 13 and Fig. 14. Fig. 13 shows a high resolution flexible circuit

board on photopaper substrate, thin lines with high conductivity were successfully deposited on its surface. Fig. 14 is an integrated test pattern for the printed electronics, there are several essential circuits' elements in this pattern such as micro antenna, thin film capacitors, straight lines with different width and connecting board. Fig. 15 and Fig. 16 are the microscope images of the printed copper circuits. Fig. 15 is a part of the circuit board, we can see that the smallest feature size is almost down to ~50 microns. A part of a micro inductive coil is shown in Fig.16 with a feature size down to ~75 microns. Saw tooth can be observed in the image which is caused by little displace of the printhead in order to create a cure line instead of a straight line.

A 3M # 600 tape was adopted to test the adhesion, no peeling off was observed after three times tearing down, indicating a very strong adhesion between the copper and the photopaper substrate. The tape test showed almost no influence on the conductivity (decrement rate less than 1%) of patterns before/after sintering. Patterns with a feature size up to ~50 μm is shown in Fig. 13, Fig. 14, revealing a well aligned high resolution copper circuit, presenting the functional integrated circuit fabricated by this method, which remains in function under deformation.

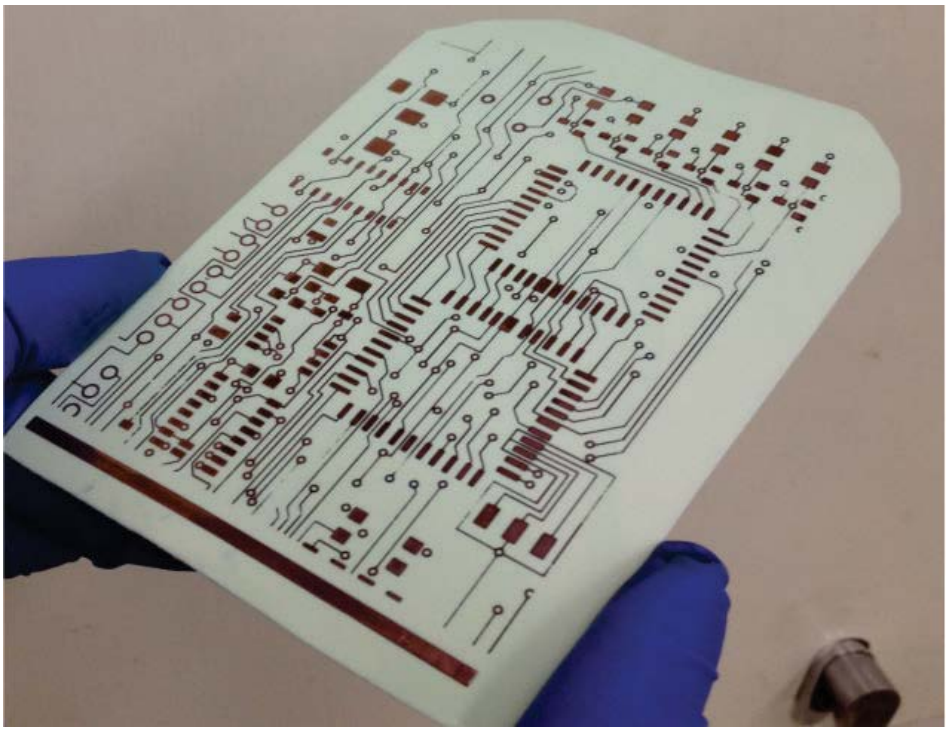

Figure 13: High resolution complex flexible circuit board on photopaper

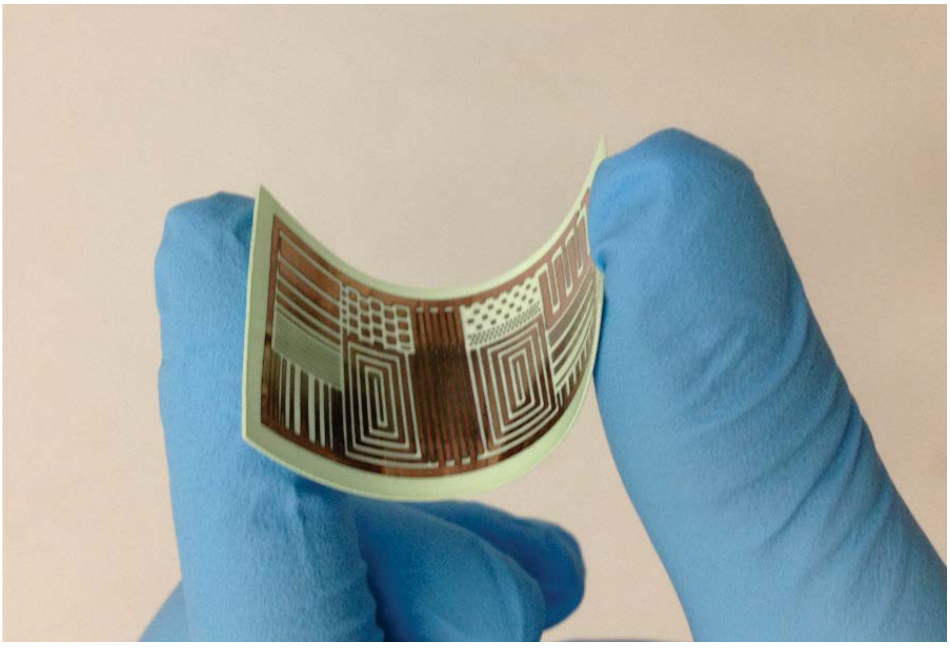

Figure 14: Integrated test pattern of the new printed electronics fabrication method

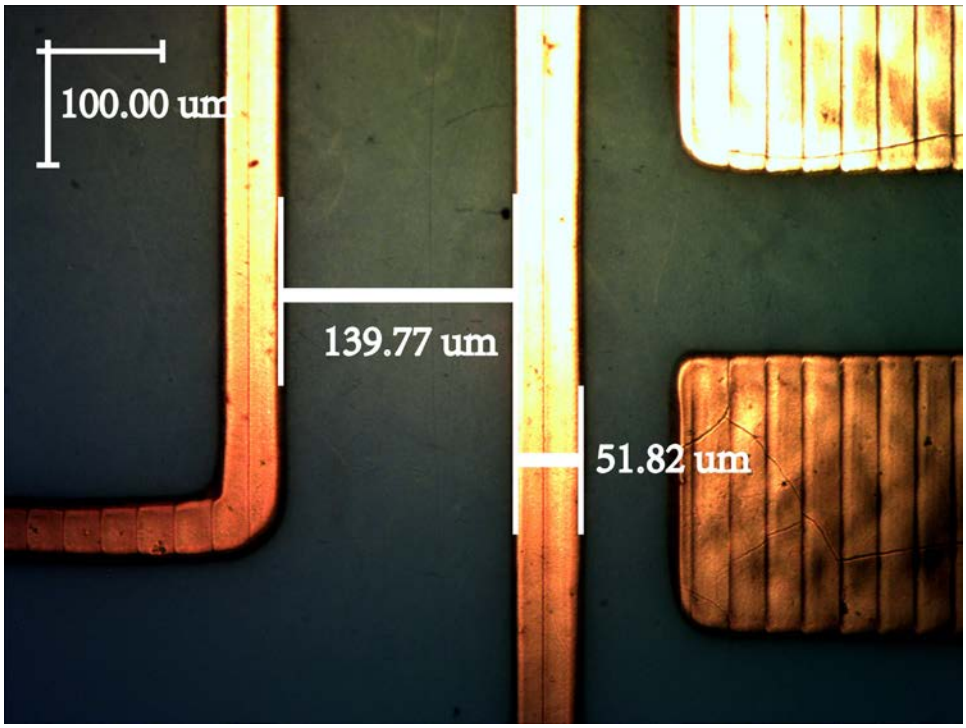

Figure 15: Microscope image of a part of the high resolution printed circuit board

Figure 16: Microscope image of a part of micro inductive coil fabricated by the proposed method

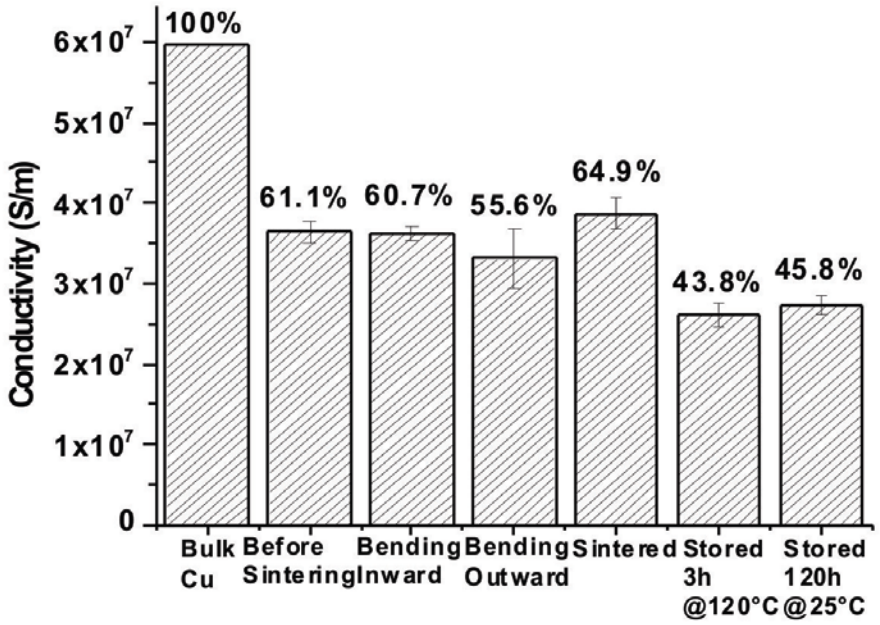

Figure 17: Conductivity measurement results of patterns under different conditions by four-probe method (bending curvature 1 cm^{-1})

Generally, a sintering process is needed for patterns fabricated by directly inkjet printing metal particles on substrates, to render the pattern and make it conductive. Because of the large surface area of the nanoparticles, the melting point becomes lower than bulk metal, thus usually ~200 ^{o}C will make the metal particles on the surface melt and connect with each other. While the patterns fabricated using our method have already showed a very good conductivity even before the sintering process, which means sintering is not that necessary. . But we still conducted the sintering experiments to see if there will be any improvement in conductivity or any other influence on the circuits. We also conducted the stability test of the copper patterns which were partly stored in open air for 120 days under room temperature and partly heated up to 120 ^{o}C for three hours also in open air. The conductivity was measured using a four-probe method and the results are all shown

in Fig. 17. For the bending conductivity test, we adopted the radius of curvature of 1 cm^{-1} for both the inward and outward bending. We kept the bending for one hour and measured the conductivity in real time by a four-probe station. The results shown in Fig.17 is the average conductivity of the patterns under bending condition. Actually there was no obvious change in the conductivity during the one hour of bending test. From Fig. 17 we can see that the copper lines have already shown good conductivity up to 3.6 x 10^7 S/m before sintering. The high conductivity achieved here can be attributed to the abundant metal ions in the ELD copper plating bath, resulting in dense uniform copper layer with good conductivity.

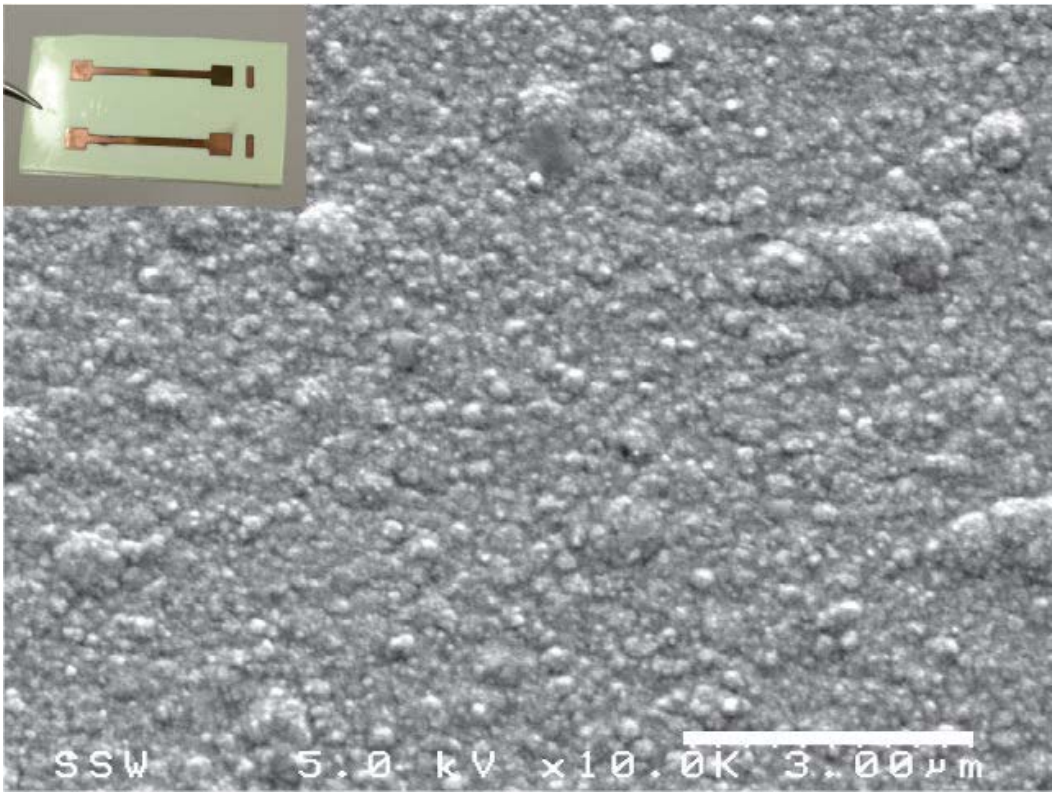

Figure 18: SEM image of un-sintered copper pattern on photopaper substrate

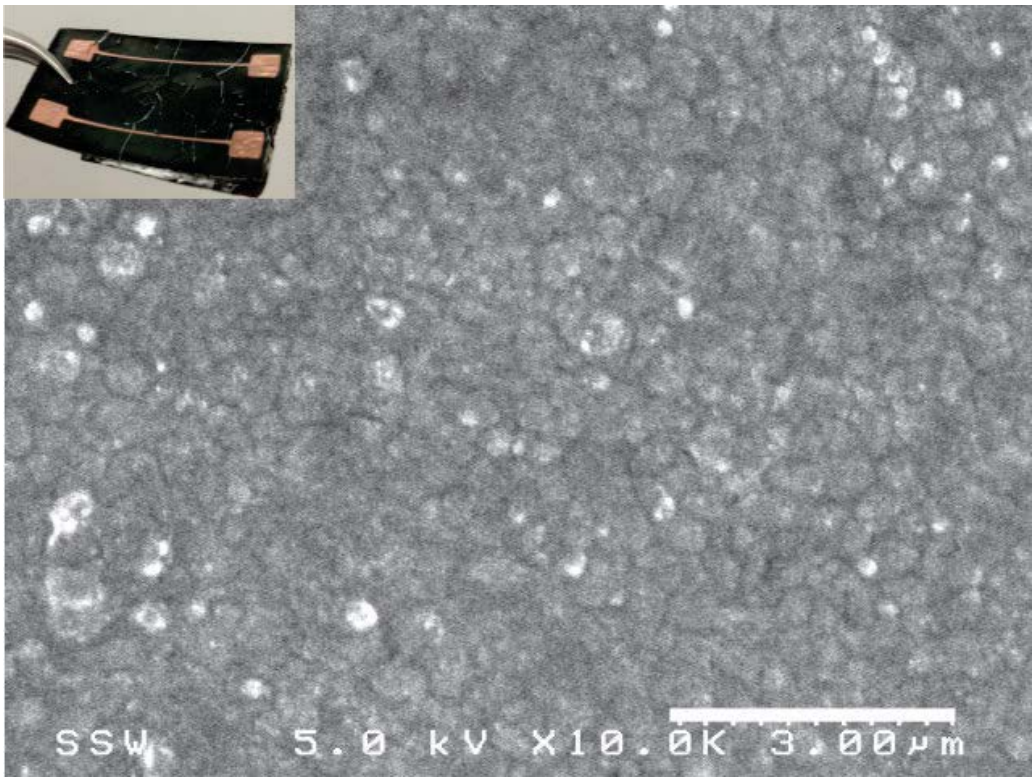

Figure 19: SEM image of sintered copper pattern on photopaper substrate

SEM and AFM were also taken to observe the surface structure of both the sintered and un-sintered patterns (Fig. 18, Fig. 19). Clusters of copper particles can be clearly observed before sintering (Fig. 18). Fig. 19 is the surface of the pattern after taking one hour thermal sintering under nitrogen flow, in which no copper particles are observed, leading to an slightly increment (about 4%, Fig. 17) in the conductivity. We also tested the conductivity of the patterns under deformation, results showed that the inward bending has little impact on the conductivity while an outward bending can lead to a ~6% decrement on its conductivity, caused by some tiny cracking on the surface. The decrement is reversible, when the patterns restore to its original shape, the conductivity will then increase to ~95% of its initial value. To test the stability of the deposited copper, we put the sample on a hot plate heating up to 120 ^{o}C in air for 12 hours, and measured

its conductivity every 20 mins. Three hours later the conductivity tended to be stable and kept its level (~43.8%) for the rest of the time. We also measured several samples stored under room temperature for more than 180 days and results showed a ~10% decrement in its conductivity as shown in Fig.17, almost the same as the stable state of samples under 120 ^{o}C. So the conductivity of copper pattern fabricated in this way will remain the same after a ~10% rapid decrement. We have to say that the thermal sintering doesn't suit for the paper-based electronics, even though it does enhance the patterns' conductivity. After a 200 ^{o}C sintering, the paper substrate was carbonized as is shown in Fig.19 and thus showed no flexibility any more. Surface crack which may result in fatal failure of the functional circuits was also observed on the sintered patterns, limiting their application. So at this moment we decided to realize our idea on a more stable, water resistant, transparent and flexible substrate, for example PET/PI which became our next project. Details of this will be further illustrated in Chapter 3.

Roughness was measured using the AFM, the average roughness (Ra) of un-sintered copper pattern is ~50 nm while for the patterns after sintering, and the roughness reduces to only 1-2 nm, which gives explanation to the increased conductivity. The AFM 3D images (Fig. 20 and 21) show a sharp contrast between the copper layers before and after thermal sintering. Finally the copper patterns achieve a high conductivity up to 3.87 x 10^{7} S/m (65.1% of bulk copper), compared to conductivity data of inkjet-printed copper reported in literature, which typically ranges from 10% to 31% of bulk copper. [21, 46, 47]

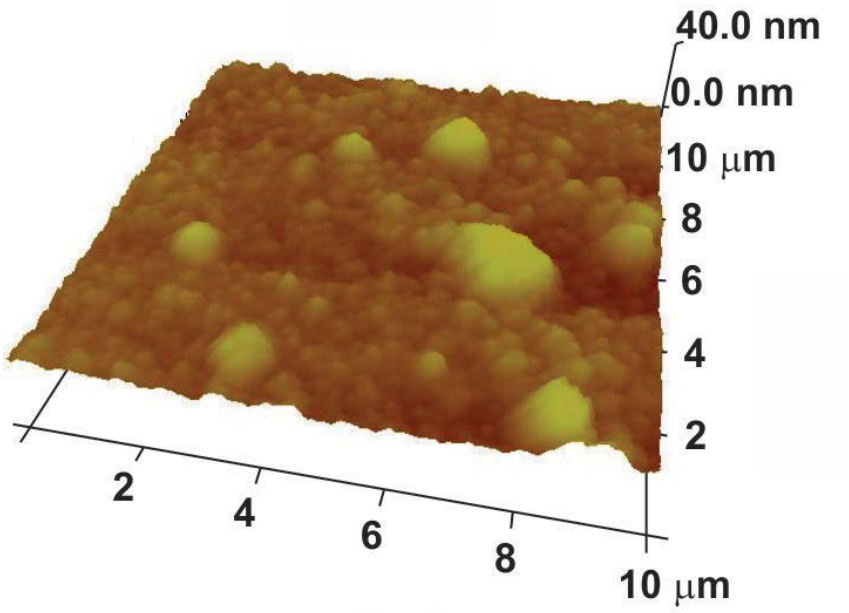

Figure 20: AFM 3D image of the copper surface (before sintering)

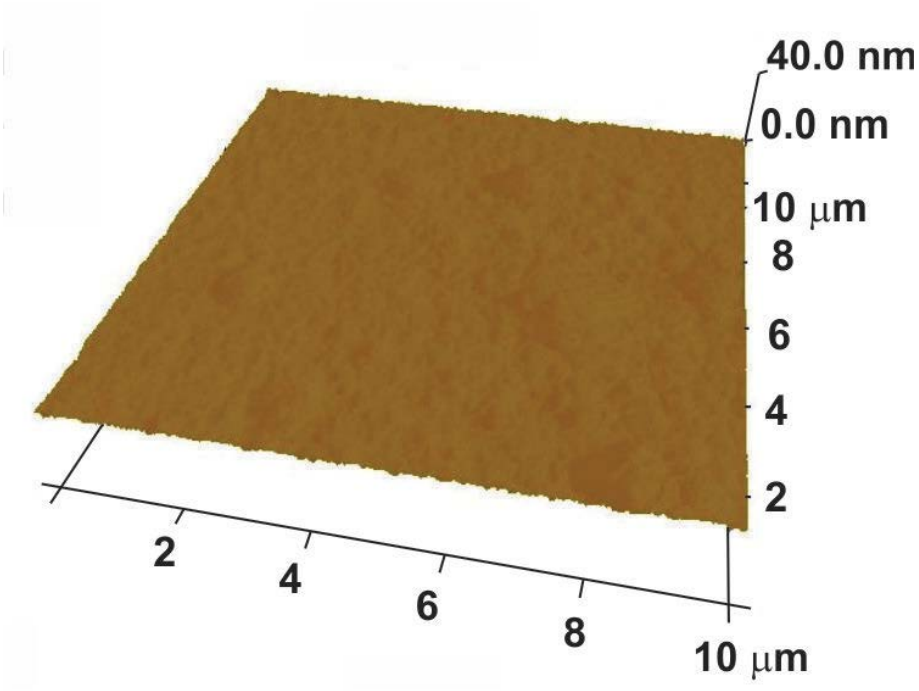

Figure 21: AFM 3D image of the copper surface (after sintering)

Compared with those copper patterns deposited on plastic substrate (PET/PI) using ELD whose conductivity can reach up to ~90% bulk, [22] the 65.1% bulk conductivity is not that impressive and the barrier for higher conductivity may be due to the photopaper substrate. To find out the reason, we conducted the AFM profile scanning for the samples of the copper on photopaper, photopaper before and after ELD bath. The results of the height information are shown in Fig. 22 and Fig.23. Many raised areas can be observed in the picture of photopaper after ELD, these raised parts were caused by ELD bath. During the ELD process, the air in between the fibers of the photopaper resulted in these raised areas and thus limited the conductivity of the patterns. These raised areas increased the roughness of the photopaper which in turn caused a relative rough surface on the bottom surface of the copper. In Fig. 23, we can see that compared with the photopaper substrate, the copper surface is much more smooth and steady, which means that the actual average thickness is less than that shown in Fig. 12. All these contributed to the loss of the conductivity. X-ray diffraction was conducted to study the crystalline structures of the resultant copper layer (under 40kV/40mA, X-Ray, continuous scanning mode, 2 deg./min. scan speed, 0.02 deg. step width, 5-90 deg. scan range, fixed monochord.) Fig. 24 shows the XRD patterns of copper patterns deposited on photopaper. For reference, the substrate photopaper was also conducted XRD measurement. Both the samples before and after sintering shows two characteristic peaks for metallic copper crystalline at 43^{o} and 51^{o} presenting for the Bragg's reflection indices of (111) and (200) planes in FCC structure. Both of the characteristic peaks became higher and more narrow after sintering (Fig. 24), indicating a finer crystal structure of the deposited copper.

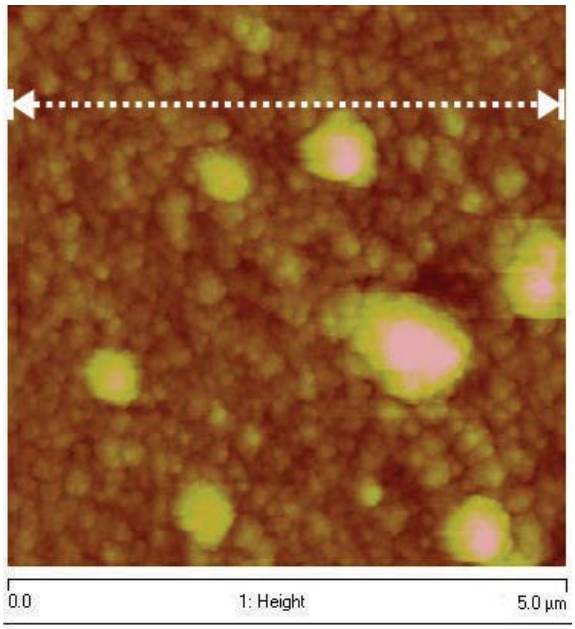

Copper

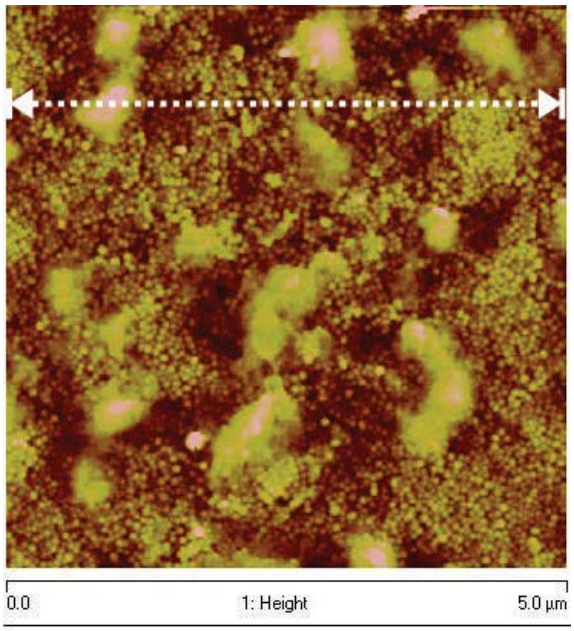

Photopaper after ELD

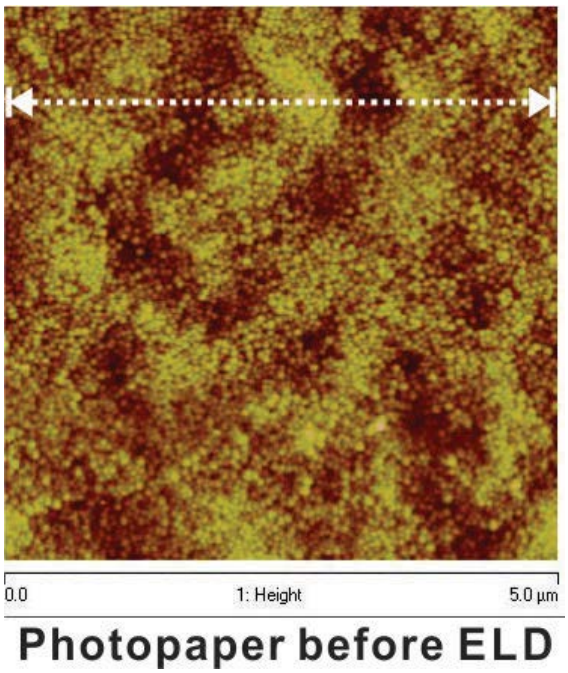

Figure 22: AFM height information images of copper (before sintering), photopaper after ELD bath and photopaper before ELD

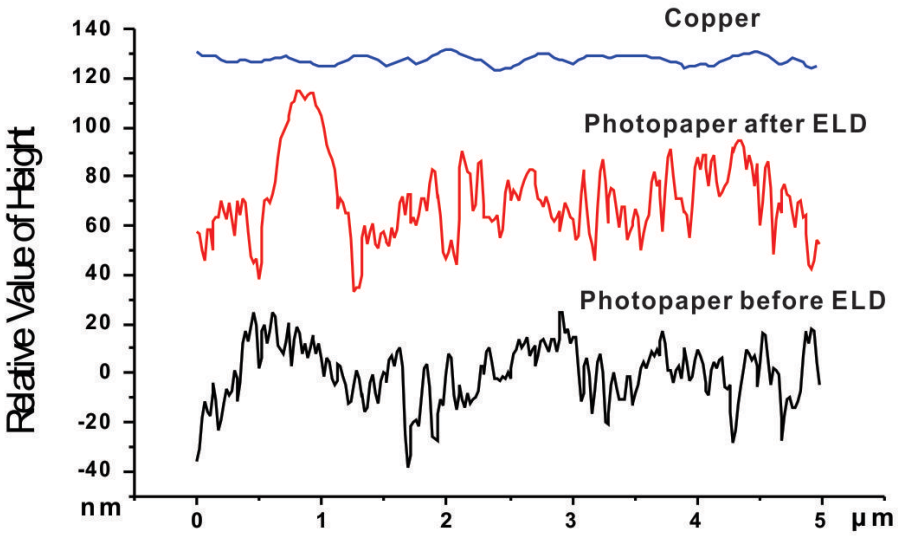

Figure 23: AFM Section profile of selected parts showing in Fig. 22 with white dash lines, corresponding to the copper, photopaper after ELD and photopaper before ELD one by one.

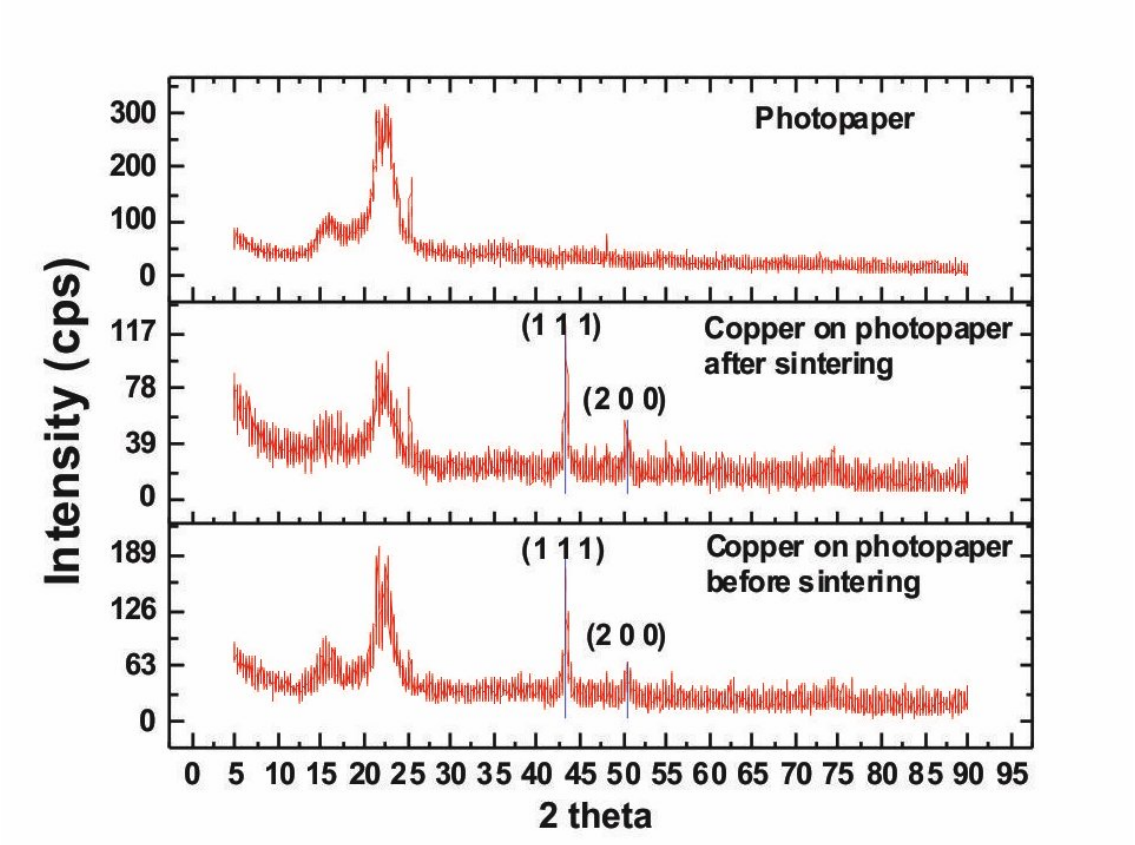

Figure 24: XRD patterns of photopaper, copper on photopaper after sintering and copper on photopaper before sintering

2.5 Conclusion

In this project, we've successfully developed a new method of fabricating flexible printed electronics. The new method was successfully adopted to fabricate high-resolution copper pattern with high conductivity and feature dimensions down to ~50 μm on photopaper substrate using inkjet printing and ELD techniques, solving many critical issues of the fabrication of the printed electronics. A stabilized palladium (II) solution in water/glycerol with optimized viscosity and concentration was prepared enabling strong chemical bonds between the quaternary ammonium groups on the photopaper and the palladium ions, leading to a strong copper adhesion. Cost-effective procedure and

chemicals were involved, eliminating issues generally associated with ink sediment, nozzle clog and stability, creating well sintered, defect free copper pattern with enhanced conductivity (65% of bulk). The feasible method based on inkjet printing is clearly demonstrated by fabricating complex functional circuits, providing a competitive manufacturing process for future printed electronics industry.

We achieved objective 1 but we also found new problem. As is mentioned before, the photopaper substrate has many limitations and the fibre properties of the paper reduce the conductivity of the deposited copper in some extent. So we decided to make it on a polymer based substrate, for example PET. While for PET substrate, it's hard to have it treated using conventional surface treating method because of its chemical inertness, and what's more, to get it treated by conventional wet chemical method a lot of toxic and hazardous chemicals and solution will be involved. You may asked that why you need to get it treated? Well, if not, there is no possibility for the ink or deposited copper staying on the PET surface, which means the adhesion is very weak and metal layers on the surface will easily peel off. That is unacceptable for printed electronics. Thus, based on the same idea of fabricating printed electronics, we tried to develop a new surface treating method enabling a high conductivity, strong adhesion copper circuits on PET substrate. The method will be further illustrated in Chapter 3.

2.6 References

[1] C. Wagner and N. Harned, "EUV LITHOGRAPHY Lithography gets extreme," *Nature Photonics*, vol. 4, pp. 24-26, Jan 2010.

[2] Y. F. Zhang, H. J. Geng, Z. H. Zhou, J. Wu, Z. M. Wang, Y. Z. Zhang, *et al.*, "Development of Inorganic Solar Cells by Nanotechnology," *Nano-Micro Letters*, vol. 4, pp. 124-134, Jun 2012.

[3] X. Li, G. Wang, X. Wang, X. Li, and J. Ji, "Flexible supercapacitor based on MnO2 nanoparticles via electrospinning," *Journal of Materials Chemistry A*, vol. 1, pp. 10103-10106, 2013.

[4] J. Perelaer, P. J. Smith, D. Mager, D. Soltman, S. K. Volkman, V. Subramanian, *et al.*, "Printed electronics: the challenges involved in printing devices, interconnects, and contacts based on inorganic materials," *Journal of Materials Chemistry*, vol. 20, pp. 8446-8453, 2010.

[5] X. Wang, T. Li, J. Adams, and J. Yang, "Transparent, stretchable, carbon-nanotube-inlaid conductors enabled by standard replication technology for capacitive pressure, strain and touch sensors," *Journal of Materials Chemistry A*, vol. 1, pp. 3580-3586, 2013.

[6] D. Lupo, W. Clemens, S. Breitung, and K. Hecker, "OE-A Roadmap for Organic and Printed Electronics," in *Applications of Organic and Printed Electronics*, E. Cantatore, Ed., ed: Springer US, 2013, pp. 1-26.

[7] A. Teichler, J. Perelaer, and U. S. Schubert, "Inkjet printing of organic electronics - comparison of deposition techniques and state-of-the-art developments," *Journal of Materials Chemistry C*, vol. 1, pp. 1910-1925, 2013.

[8] A. R. Uhl, C. Fella, A. Chirila, M. R. Kaelin, L. Karvonen, A. Weidenkaff, *et al.*, "Non-vacuum deposition of Cu(In,Ga)Se2 absorber layers from binder free, alcohol solutions," *Progress in Photovoltaics*, vol. 20, pp. 526-533, Aug 2012.

[9] S. Ito and Y. Mikami, "Porous carbon layers for counter electrodes in dye-sensitized solar cells: Recent advances and a new screen-printing method," *Pure and Applied Chemistry*, vol. 83, pp. 2089-2106, Aug 2011.

[10] T. T. Nge, M. Nogi, and K. Suganuma, "Electrical functionality of inkjet-printed silver nanoparticle conductive tracks on nanostructured paper compared with those on plastic substrates," *Journal of Materials Chemistry C*, vol. 1, pp. 5235-5243, 2013.

[11] C. Newby, J.-K. Lee, and C. K. Ober, "Inkjet printing of fluorinated materials and their application to patterning organic semiconductors," *Journal of Materials Chemistry C*, vol. 1, pp. 5647-5653, 2013.

[12] Y. Yang, T. Nakamichi, H. Yoshioka, M. Yahiro, M. Era, H. Watanabe, *et al.*, "Spectral-resolving capable and integratable multilayered conductive films via an inkjet method," *Journal of Materials Chemistry C,* vol. 1, pp. 1739-1744, 2013.

[13] T. Xu, W. X. Zhao, J. M. Zhu, M. Z. Albanna, J. J. Yoo, and A. Atala, "Complex heterogeneous tissue constructs containing multiple cell types prepared by inkjet printing technology," *Biomaterials,* vol. 34, pp. 130-139, Jan 2013.

[14] S. Y. Cho, J. M. Ko, J. Lim, J. Y. Lee, and C. Lee, "Inkjet-printed organic thin film transistors based on TIPS pentacene with insulating polymers," *Journal of Materials Chemistry C,* vol. 1, pp. 914-923, 2013.

[15] S. Jeong, S. H. Lee, Y. Jo, S. S. Lee, Y.-H. Seo, B. W. Ahn, *et al.*, "Air-stable, surface-oxide free Cu nanoparticles for highly conductive Cu ink and their application to printed graphene transistors," *Journal of Materials Chemistry C,* vol. 1, pp. 2704-2710, 2013.

[16] H. H. Chen, R. Anbarasan, L. S. Kuo, M. Y. Tsai, P. H. Chen, and K. F. Chiang, "Synthesis, characterizations and hydrophobicity of micro/nano scaled heptadecafluorononanoic acid decorated copper nanoparticle," *Nano-Micro Letters,* vol. 2, pp. 101-105, May 2010.

[17] X. Q. Liu, X. C. Zhou, Y. Li, and Z. J. Zheng, "Surface-Grafted Polymer-Assisted Electroless Deposition of Metals for Flexible and Stretchable Electronics," *Chemistry-an Asian Journal,* vol. 7, pp. 862-870, May 2012.

[18] X. Wang, T. Zhang, B. Kobe, W. M. Lau, and J. Yang, "Grafting of polyelectrolytes onto hydrocarbon surfaces by high-energy hydrogen induced cross-linking for making metallized polymer films," *Chem Commun (Camb),* vol. 49, pp. 4658-60, May 2013.

[19] R. S. Guo, Y. Yu, Z. Xie, X. Q. Liu, X. C. Zhou, Y. F. Gao, *et al.*, "Matrix-Assisted Catalytic Printing for the Fabrication of Multiscale, Flexible, Foldable, and Stretchable Metal Conductors," *Advanced Materials,* vol. 25, pp. 3343-3350, Jun 2013.

[20] X. L. Wang, H. Hu, Y. D. Shen, X. C. Zhou, and Z. J. Zheng, "Stretchable Conductors with Ultrahigh Tensile Strain and Stable Metallic Conductance Enabled by Prestrained Polyelectrolyte Nanoplatforms," *Advanced Materials,* vol. 23, pp. 3090-3094, Jul 2011.

[21] B. K. Park, D. Kim, S. Jeong, J. Moon, and J. S. Kim, "Direct writing of copper conductive patterns by ink-jet printing," *Thin Solid Films,* vol. 515, pp. 7706-7711, Jul 2007.

[22] C. Y. Kao and K. S. Chou, "Electroless copper plating onto printed lines of nanosized silver seeds," *Electrochemical and Solid State Letters,* vol. 10, pp. D32-D34, 2007.

[23] X. Q. Liu, H. X. Chang, Y. Li, W. T. S. Huck, and Z. J. Zheng, "Polyelectrolyte-Bridged Metal/Cotton Hierarchical Structures for Highly Durable Conductive Yarns," *Acs Applied Materials & Interfaces,* vol. 2, pp. 529-535, Feb 2010.

[24] D. Zabetakis and W. J. Dressick, "Statistical Analysis of Plating Variable Effects on the Electrical Conductivity of Electroless Copper Patterns on Paper," *Acs Applied Materials & Interfaces,* vol. 4, pp. 2358-2368, May 2012.

[25] Q. Ye, X. L. Wang, H. Y. Hu, D. A. Wang, S. B. Li, and F. Zhou, "Polyelectrolyte Brush Templated Multiple Loading of Pd Nanoparticles onto TiO2 Nanowires via Regenerative Counterion Exchange-Reduction," *Journal of Physical Chemistry C,* vol. 113, pp. 7677-7683, May 7 2009.

[26] M. Okano, T. Inoue, Y. Takizawa, T. Matsuda, and A. Miyao, "A New Nozzle for Continuous Inkjet Printers," *Journal of Advanced Mechanical Design, Systems, and Manufacturing,* vol. 4, pp. 764-772, 2010.

[27] L. J. Durney, *Graham's Electroplating Engineering Handbook*: Springer, 1984.

[28] A. Cahill, "Surface catalyzed reduction of copper," *Proc. Am. Electroplaters' Soc,* vol. 44, p. 130, 1957.

[29] F. W. Schneble, "Electroless copper plating," ed: Google Patents, 1967.

[30] F. Hanna, Z. A. Hamid, and A. A. Aal, "Controlling factors affecting the stability and rate of electroless copper plating," *Materials Letters,* vol. 58, pp. 104-109, 2004.

[31] G. Devaraj, S. Guruviah, and S. Seshadri, "Pulse plating," *Materials Chemistry and physics,* vol. 25, pp. 439-461, 1990.

[32] V. Lim, E. Kang, and K. Neoh, "Electroless plating of palladium and copper on polypyrrole films," *Synthetic metals,* vol. 123, pp. 107-115, 2001.

[33] M. F. Mabrook, C. Pearson, and M. C. Petty, "Inkjet-printed polymer films for the detection of organic vapors," *Ieee Sensors Journal,* vol. 6, pp. 1435-1444, Dec 2006.

[34] S. Cerimovic, R. Beigelbeck, H. Antlinger, J. Schalko, B. Jakoby, and F. Keplinger, "Sensing viscosity and density of glycerol–water mixtures utilizing a suspended plate MEMS resonator," *Microsystem Technologies,* vol. 18, pp. 1045-1056, Aug 2012.

[35] Y. F. Liu, M. H. Tsai, Y. F. Pai, and W. S. Hwang, "Control of droplet formation by operating waveform for inks with various viscosities in piezoelectric inkjet printing," *Applied Physics a-Materials Science & Processing,* vol. 111, pp. 509-516, May 2013.

[36] L. Jacot-Descombes, M. Gullo, V. Cadarso, and J. Brugger, "Fabrication of epoxy spherical microstructures by controlled drop-on-demand inkjet printing," *Journal of Micromechanics and Microengineering,* vol. 22, p. 074012, 2012.

[37] Y.-H. Chang and C.-H. Wang, "Electroless deposition of Cu nanostructures on molecular patterns prepared by dip-pen nanolithography," *Journal of Materials Chemistry,* vol. 22, pp. 3377-3382, 2012.

[38] S. Busato, A. Belloli, and P. Ermanni, "Inkjet printing of palladium catalyst patterns on polyimide film for electroless copper plating," *Sensors and Actuators B-Chemical,* vol. 123, pp. 840-846, May 2007.

[39] H. C. Koo, C. Lightsey, and P. A. Kohl, "Affect of Anneal Temperature on All-Copper Flip-Chip Connections Formed via Electroless Copper Deposition," *Ieee Transactions on Components Packaging and Manufacturing Technology,* vol. 2, pp. 79-84, Jan 2012.

[40] C. Yang, C. P. Wong, and M. M. F. Yuen, "Printed electrically conductive composites: conductive filler designs and surface engineering," *Journal of Materials Chemistry C,* vol. 1, pp. 4052-4069, 2013.

[41] A. Definitions, "A Compilation of ASTM Standard Definitions," ed: ASTM, Philadelphia, 1994.

[42] F. Hanna, Z. A. Hamid, and A. A. Aal, "Controlling factors affecting the stability and rate of electroless copper plating," *Materials Letters,* vol. 58, pp. 104-109, Jan 2004.

[43] L. Chen, M. Crnic, Z. H. Lai, and J. H. Liu, "Process development and adhesion behavior of electroless copper on liquid crystal polymer (LCP) for electronic packaging application," *Ieee Transactions on Electronics Packaging Manufacturing,* vol. 25, pp. 273-278, Oct 2002.

[44] L. I. Elding, "Palladium(II) halide complexes. I. Stabilities and spectra of palladium(II) chloro and bromo aqua complexes," *Inorganica Chimica Acta,* vol. 6, pp. 647-651, Jun 1972.

[45] A. A. Khalate, X. Bombois, G. Scorletti, R. Babuška, S. Koekebakker, and W. De Zeeuw, "A waveform design method for a piezo inkjet printhead based on robust feedforward control," 2012.

[46] S. Jeong, K. Woo, D. Kim, S. Lim, J. S. Kim, H. Shin, *et al.*, "Controlling the thickness of the surface oxide layer on Cu nanoparticles for the fabrication of conductive structures by ink-jet printing," *Advanced Functional Materials,* vol. 18, pp. 679-686, Mar 2008.

[47] J. Cheon, J. Lee, and J. Kim, "Inkjet printing using copper nanoparticles synthesized by electrolysis," *Thin Solid Films,* vol. 520, pp. 2639-2643, Jan 2012.

Chapter 3

3 Fabrication of high conductivity flexible copper patterns on PET

In this chapter, a method of fabricating high conductivity copper pattern on PET is demonstrated, corresponding to the objective 2. Polyelectrolytes were grafted to hydrocarbon surfaces by selective cleavage of C-H bonds using hyperthermal hydrogen with properly controlled kinetic energy to develop high quality metalized polymer patterns via electroless deposition, which presents excellent conductivity and adhesion between metal layer and substrate, pushing the board of the printed electronics forward again.

3.1 Introduction

Metallized polymer patterns further enrich the properties of light-weight, flexible polymers with additional properties that are usually associated with metals, such as electrical conductivity, reflectivity, abrasion resistance, etc., which are highly suitable for the printed circuit boards, microelectronics industry, and rising flexible and stretchable electronics. [1, 2] Electroless deposition (ELD) has recently emerged as a versatile and cost-effective tool to manufacture high quality metal structures. ELD can form metal films on surfaces in the presence of catalysts, usually surface-immobilized metal cations, via an autocatalytic redox reaction at room temperature. The abundant metal ions in the ELD solution result in dense and uniform deposited layer on the substrate with high conductivity. So we adopted this technique to fabricated high quality printed electronics, as is illustrated in Chapter 2. The ELD process is especially suitable for polymer substrates that could not survive at the high temperature required for vapor deposition

approaches. [3]

Very recently, a strategy for catalyst immobilization by surface-grafted polyelectrolytes has attracted increasing interest due to its ability to produce metal structures with high spatial resolution. The key of this method is the polyelectrolyte anchoring layer for catalyst uptake, which can not only provide a large number of binding sites along the polymer chains for catalyst uptake, resulting in high ELD efficiency, but also dramatically enhance adhesion and mechanical stability by forming an interpenetrating network with the deposited metal particles in ELD. [4] Several surface grafting technologies, including wet chemistry methods and physical treatments, have been employed to graft polyelectrolytes onto polymeric substrates for ELD, such as surface-initiated atom transfer polymerization, [5, 6] solution polymerization, [7-9] and UV-, radiation-, and plasma-induced polymerization. [10-12] However, for the wet chemistry methods, even the well-known SI-ATRP, which has been recognized as a green chemical approach for polymer synthesis, [13, 14] are time-consuming, produce low yields and, require inert protection during the synthetic process or chemical activation of the surfaces prior to use. What's more, they are not environmentally friendly. Especially for those polymer based substrates such PET/PI which are chemically inert, conventional surface modification method doesn't work very well. Thus, wet chemistry methods have low-throughput and high-cost, which make it difficult for large scale production and are unacceptable in the field of printed electronics. While for various physical treatments, despite of their advantages of more cost-efficiency than wet chemistry methods and substrate independence, the hot electrons, ion, radicals, and plasma etc. could cause undesirable surface functionalities, surface charges, or partial surface destruction. A dry-

process and chemical-free approach, named as hyperthermal hydrogen induced cross-linking (HHIC), has been recently developed, offers another option for grafting polymer to hydrocarbon based substrates. [15-20]

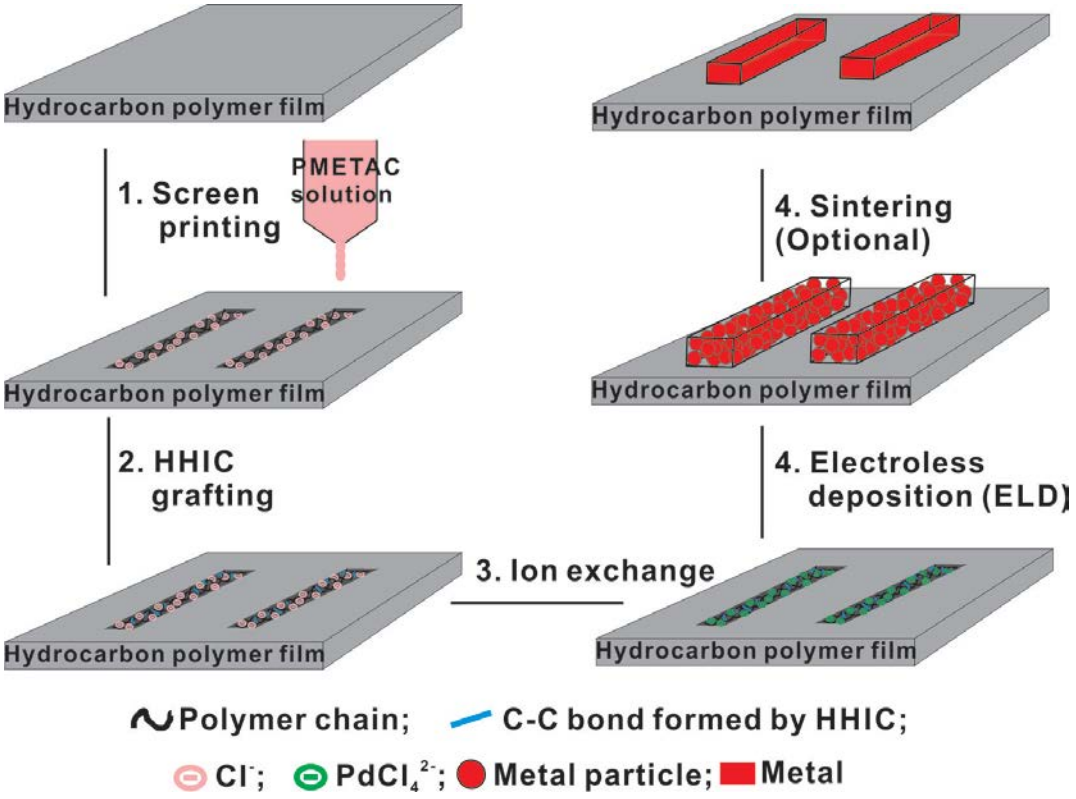

Figure 25: Schematic of polyelectrolyte molecules (PMETAC in this case) grafting to hydrocarbon surface by HHIC followed by ELD to create high quality copper patterns on PET substrate

In this chapter, we demonstrate the application of HHIC for grafting of polyelectrolytes to polymeric surfaces for metalized polymer patterns via ELD, combined with the new method of fabricating high quality electronics that we proposed in Chapter 2, flexible copper patterns were successfully fabricated on PET substrate. Fig. 25 shows the schematic of the whole process. The hyperthermal hydrogen neutrals selectively cleave C-H bonds of the polyelectrolytes and hydrocarbon surface, generating numerous carbon

radicals, which results in cross-linking of polyelectrolytes and covalent bonding of polyelectrolytes to the surface. As a proof-of-concept, poly (2-(methacryloyloxy) ethyl trimethylammo-nium chloride) (PMETAC), PET film and screen printing technique were chosen to demonstrate the process.

3.2 Theory

3.2.1 Hyperthermal hydrogen induced cross-linking (HHIC)

The concept of HHIC is based on collision kinematics. Briefly, the kinetic energy of a lightweight hydrogen projectile can be transferred to the targets when it collides with the atoms of a hydrocarbon molecule. The principle of HHIC is shown in Fig. 26. According to the mass-dependent kinematic transfer mechanism, a hydrogen projectile can transfer ~90% of its kinetic energy to a hydrogen atom but less than 50% to heavier atoms such as carbon and oxygen when they collide head-on. In principal, when considering the bond dissociation energy, such hydrogen projectiles with properly controlled kinetic energy can selectively cleave C-H bonds of hydrocarbon molecules without any other bond-cleavages happening. The dissociative C-H bonds generate carbon radicals, which lead to the cross-linking of hydrocarbon molecules to each other and/or bonding to the hydrocarbon based surfaces.

The HHIC technology, with no requirement of prior activation, additives, initiators, or solvents, makes it feasible to graft macromolecules to hydrocarbon surfaces in a fast, cost-effective, and harmless matter. Indeed, HHIC is a physical and therefore green method for molecular crosslinking. More importantly, compared to other surface treatment technologies like plasma and ATRP, HHIC technology leaves no surface

charges to the substrates after treatment, which is crucial for making high quality electronics particularly semiconductor devices. Thus, we chose this method for the substrate surface treatment.

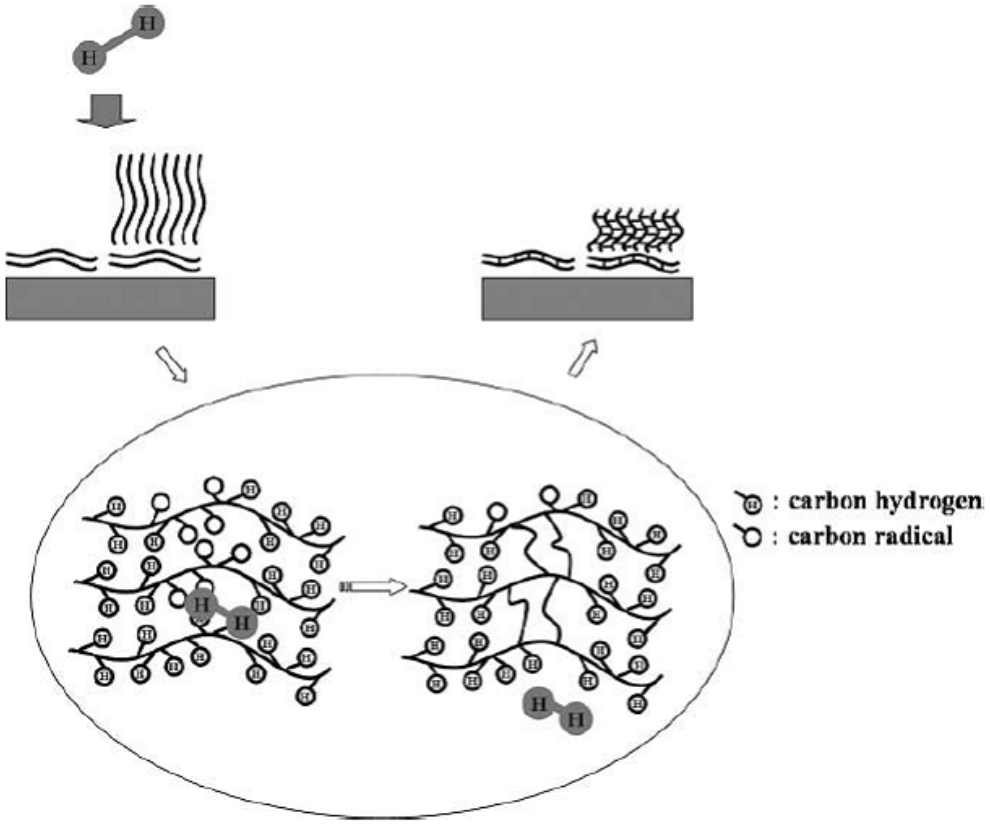

Figure 26: Schematic illustration of the mechanism of HHIC

3.3 Experiments and discussion

3.3.1 Procedure

Figure 25 shows the procedure of this printing process, which includes these steps: 1) screen printing polyelectrolyte (e.g. PMETAC) solution, where PMETAC will be firstly dissolved in ethanol and glycerol and 1,3- propanediol will be added to adjust the viscosity and surface tension; 2) grafting polyelectrolyte to the polymer substrate by

HHIC; 3) loading catalyst through ion exchange, where the samples will be immersed in $(NH_4)_2PdCl_4$ aqueous solution to load Pd moieties by ion exchange between the anions of polyelectrolyte and $PdCl_4^{2-}$; 4) electroless deposition of metals (copper) on the surface after ion exchange. As a proof-of-concept study, PET (Polyethylene terephthalate) was used as the model substrate in this project, where a shadow-mask method (screen printing method) was utilized to assist PMETAC patterning. Fig. 27 shows the HHIC and ELD procedure on a micro level, indicating the mechanism of this technique at a molecular level.

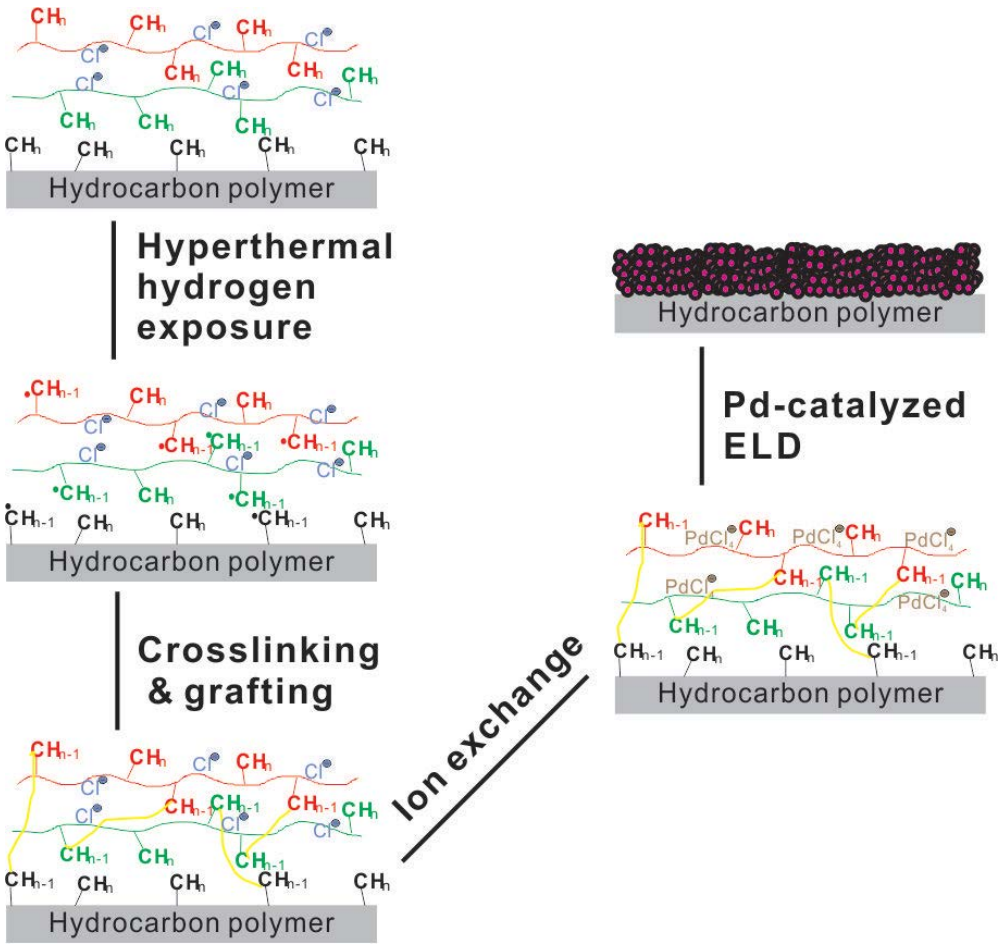

Figure 27: Schematic illustration of the proposed procedure in micro level

3.3.2 Materials

All chemicals were purchased from Aldrich and used as received. PET films 100 μm thick were purchased from Transilwrap Inc. (Canada), which were cleaned using ethanol before use. Poly (2-(methacryloyloxy)ethyl-trimethylammonium chloride) (PMETAC) was synthesized by solution polymerization of 2-(methacryloyloxy)ethyl-trimethylammonium chloride in water at 50 wt. % concentration catalyzed by 1 wt % potassium persulfate at 75 ^{o}C, which was collected by precipitation in acetone and dried in vacuum at 60 ^{o}C.

3.3.3 Fabrication of copper patterns on PET

5 mg/mL of PMETAC solution in ethanol was screen printed on the pre-cleaned PET film and air dried for 30 s. Subsequently, the samples were exposed to hyperthermal hydrogen neutrals with an extraction current of 10 mA at the pressure of 8×10^{-4} Torr to yield PMETAC grafted PET film (PMETAC-PET). [19] The HHIC treatment time was fixed at 120 s, which is sufficient time to cross-link an organic film. [21] Next, the PMETAC grafted PET composite film was immersed in a 5 mM $(NH_4)_2PdCl_4$ aqueous solution for 15 min to immobilize $PdCl_4^{2-}$ by ion exchange. $(PdCl_4)^{2-}$ will then bond on the screen printed pattern as is shown in Fig. 25. Finally, samples were immersed in a freshly prepared Cu ELD plating bath for 30 min at room temperature, resulting in the Cu coated PET. The ELD bath we used in this project was the same as that we used in project 1 (Chapter 2). The plating bath contains a 1:1 mixture of freshly prepared solutions A and B. Solution A consists of 12 g/L NaOH, 13 g/L $CuSO_4\bullet5H_2O$, and 29 g/L potassium sodium tartrate. Solution B is 9.5 mL/L HCHO in water. Please note that

copious rinses were carried out at the end of each step to avoid any physisorption of unattached chemicals.

3.3.4 Characterization

Chemical composition information about the samples was obtained by X-ray photoelectron spectroscopy (XPS). The measurement was carried out using a Kratos Axis Ultra spectrometer (shown in Fig. 28, copyright belongs to Surface Science Western, Western University) using a monochromatic Al Kα radiation source. The binding energies were referenced to the C 1s line at 284.8 eV from adventitious carbon. The morphology of copper coated PET was investigated using a Hitachi S-4500 field emission scanning electro-microscope (FESEM) using a 5 kV accelerating voltage. Atomic force microscopy (AFM) was performed on Nanoscope V (Veeco, Inc., Fig. 29) in tapping mode to characterize the surface morphology of the modified PETs and thickness of PMETAC coatings and copper films by scanning the edge of a scratch. Resistance measurements were carried out by a four-probe method using M 2400 Keithley Multimeter (shown in Fig. 30).

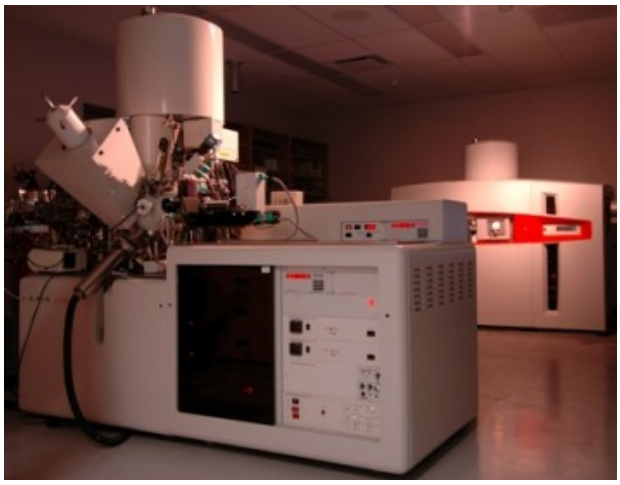

Figure 28: Kratos AXIS Ultra and AXIS Nova (Copyright: Surface Science Western, Western University)

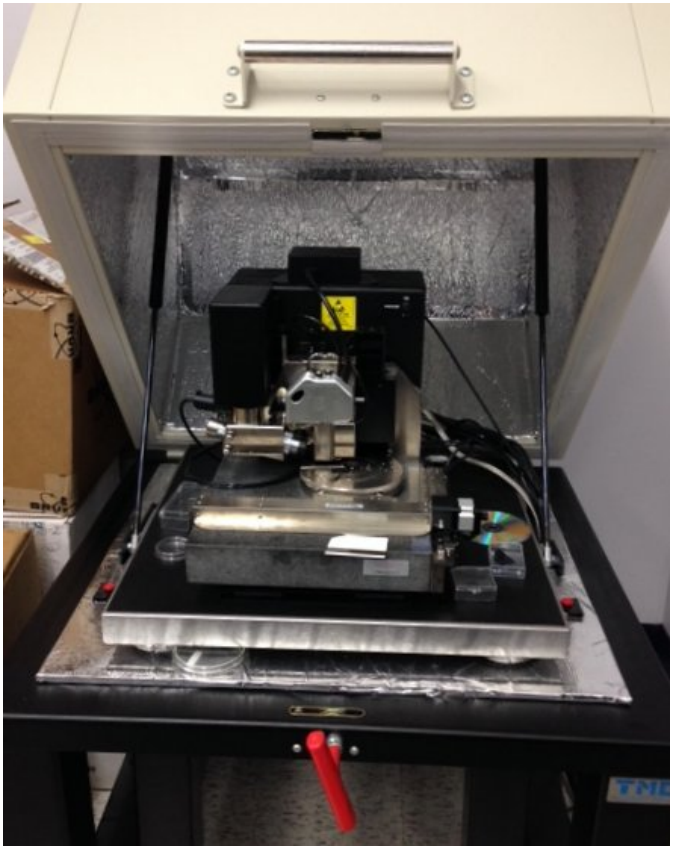

Figure 29: Nanoscope V Atomic force microscopy (AFM)

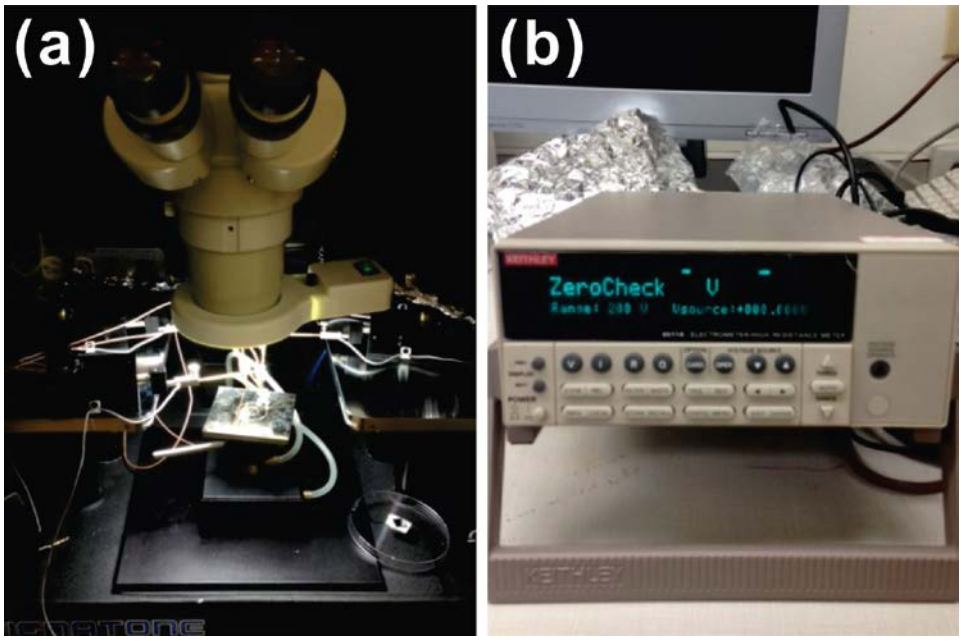

Figure 30: Conductivity measurement setup: four-probe station (a) connected to M 2400 Keithley Multimeter (b)

3.3.5 Results and discussion

The successful grafting of PMETAC to the PET film (PMETAC-PET) was confirmed by X-ray photoelectron spectroscopy (XPS). The XPS results of Cu-PET, Pd-loaded-PET, PMETAC-PET, and raw PET are shown in Fig. 31. The high resolution spectra of N 1s and Pd 3d are shown in Fig. 32 and Fig. 33 respectively. The raw PET film mainly composes of C and O (Fig. 31). After HHIC treatment, the presence of Cl and N are attributed to the formation of a PMETAC coating on PET (Fig. 32 and 33). While after ion exchange in $(NH_4)_2PdCl_4$ aqueous solution, Pd 3d5/2 and 3d3/2 signals at 340.7 eV and 335.5 eV respectively (Fig. 33) confirm the successful loading of $PdCl_4^{2-}$ moieties because of their high affinity to quaternary ammonium of PMETAC. [22] The loaded Pd moieties act as effective catalytical sites for subsequent ELD on PET. [3, 5, 6] The appearance of Cu peaks at 932.2 eV, 123.0 eV, and 75.4 eV and the complete

disappearance of N, Cl, and Pd indicate the formation of a dense copper layer after ELD, showing a high quality copper film was formed on the PET substrate.

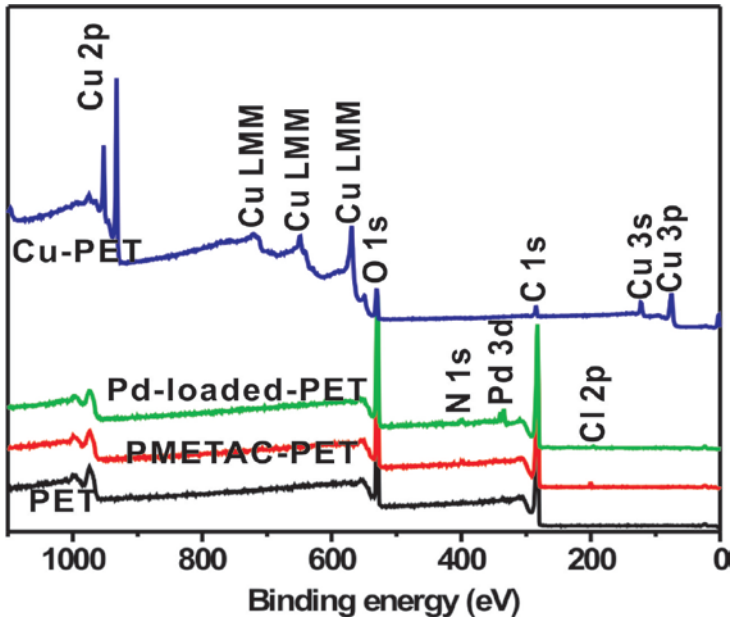

Figure 31: XPS results of Cu-PET, Pd-loaded-PET, PMETAC-PET, and raw PET

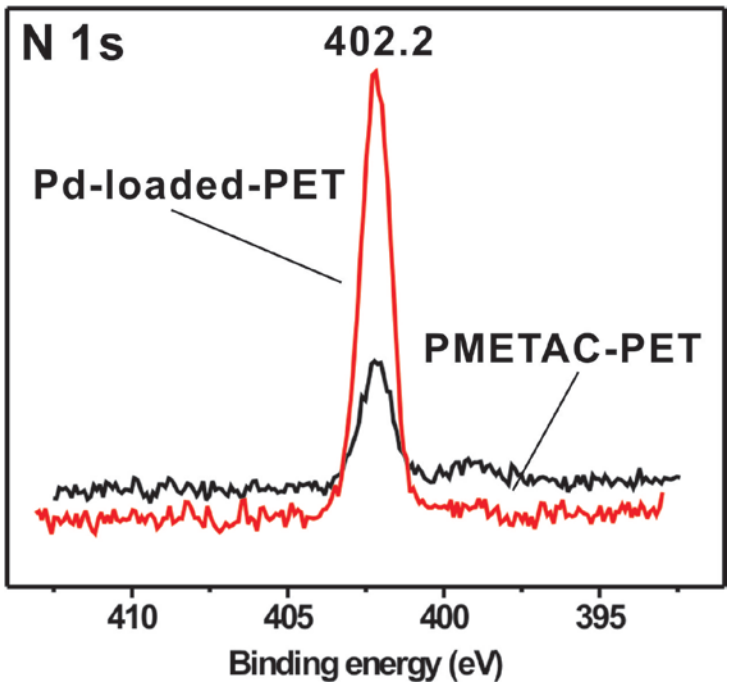

Figure 32: XPS high resolution spectra of N 1s

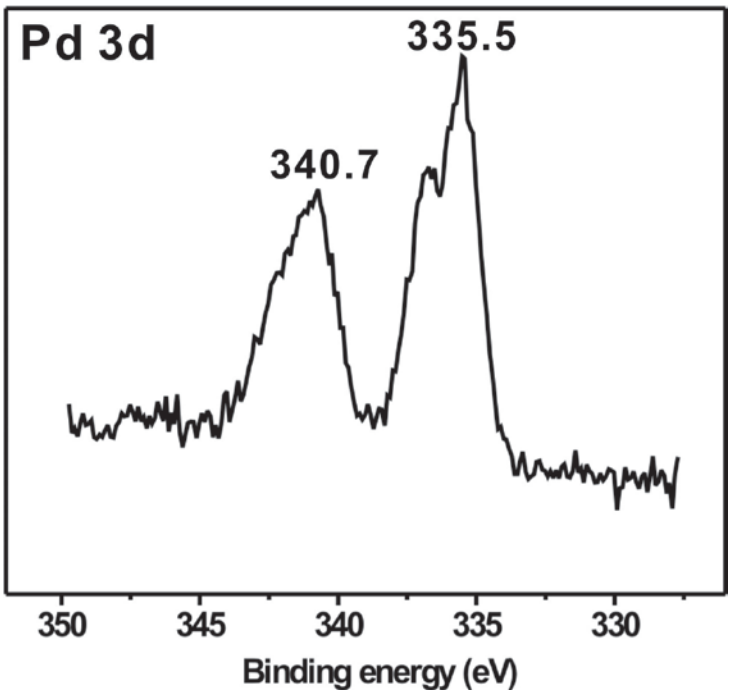

Figure 33: XPS high resolution spectra of Pd 3d

The surface morphology of the as-made PMETAC-PET and Cu-PET was observed by atomic force microscopy (AFM) and SEM. As shown in Fig. 34 - 37, it is interesting to find that the initial PET roughness (Ra) of 5.1 nm became smoother after the dense and uniform PMETAC layer was grafted, resulting in a decreased roughness of 2.4 nm. We attribute this surface smoothing to the additive manner of HHIC modification technology to the surface, which does not erase organic materials like many other physical methods since it is well controlled in hydrogen projectiles' kinetic energy. Such treatment only cleaves C-H bond, which consequently results in no increase in the roughness. [18, 19, 23] While after ELD, the copper layer formed on PET has a roughness of 4.3 nm (Fig. 36) and is composed of densely packed copper nanoparticles with c.a. 50-100 nm diameters (Fig. 37(a)). The dense Cu film, uniformly covered the entire PET surface, which is also confirmed by the scanning electron microscopy (Fig. 37(b)). These results

indicate that the present HHIC grafting technology yields uniform and defect-free PMETAC nano-coatings on the PET surface. The observed crack-free Cu layer should be a direct benefit of this uniform nano-coating. Importantly, no delamination of the as-made Cu-PET composite was observed after repeated Scotch® tape adhesion test (Fig. S1), indicating outstanding adhesion of the metal film to the substrate, which is critical for applications in electronics.

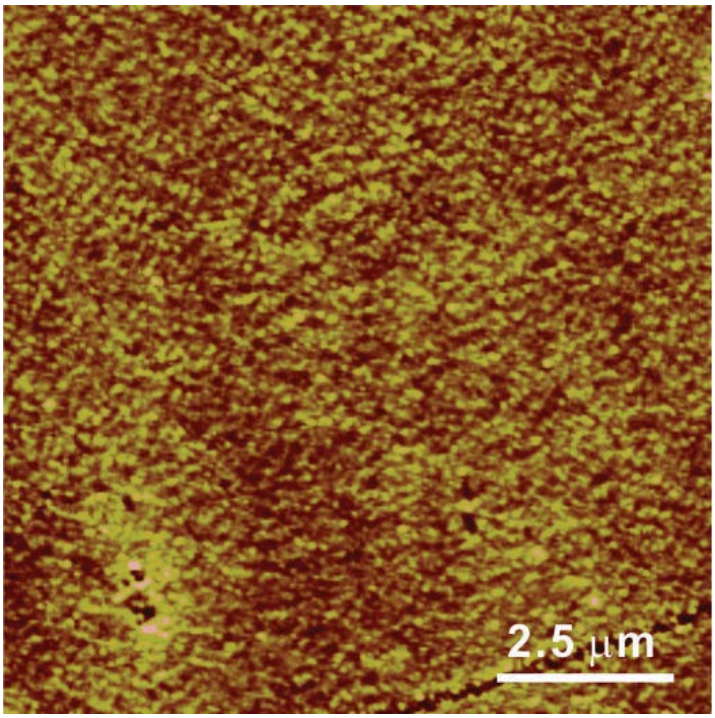

Figure 34: AFM height information of raw PET

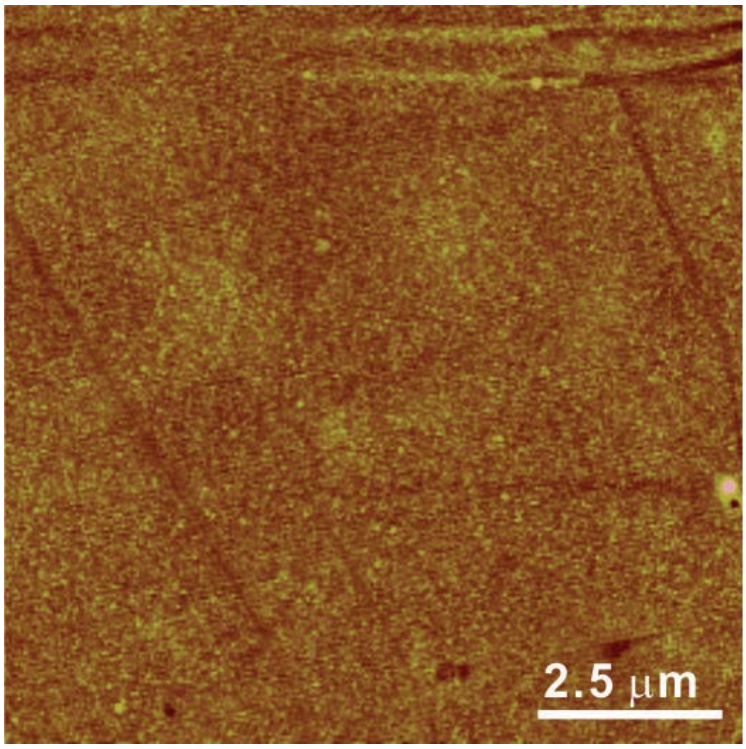

Figure 35: AFM images of PMETAC-PET

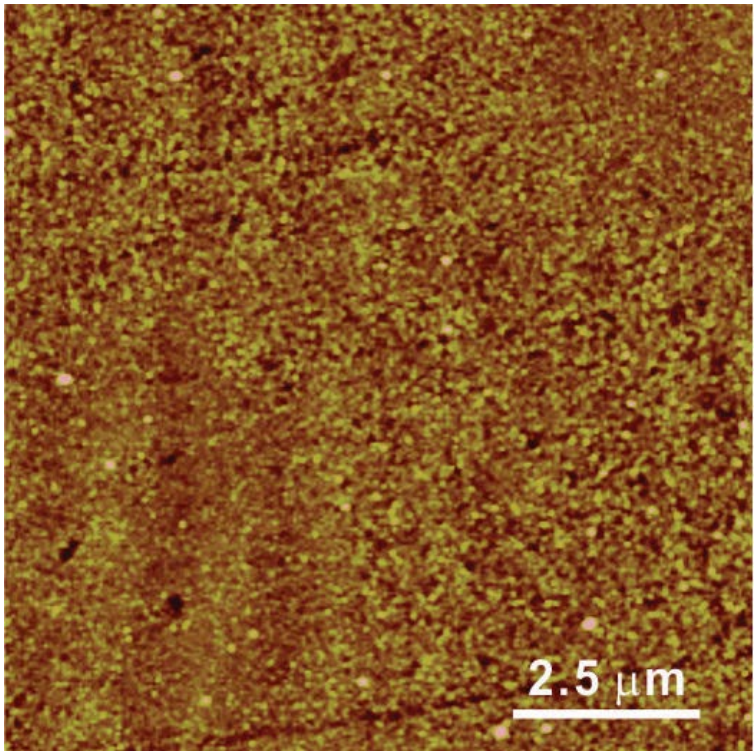

Figure 36: AFM images of Cu-PET

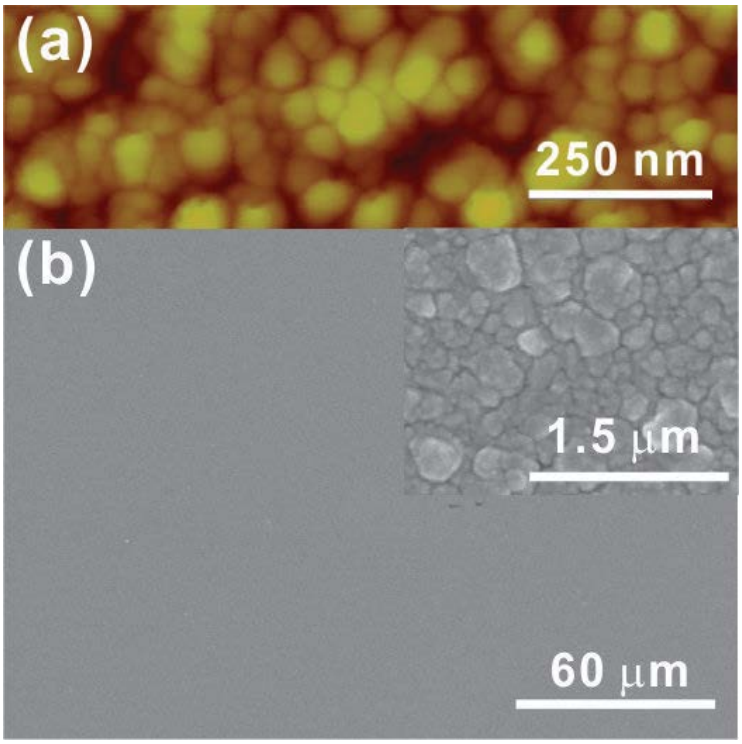

Figure 37: AFM images of Cu-PET (a), and SEM images of Cu-PET(b) in different scale

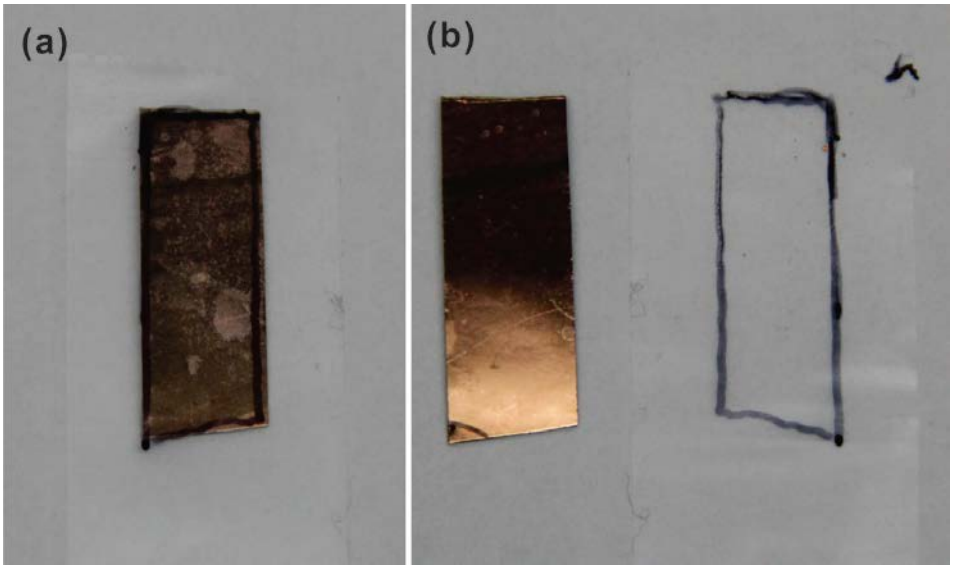

Figure 38: Photos of Scotch tape test before (a) and after (b) three times peeling-off

Normally, HHIC cross-links propagate to a depth of several nanometers, but the exact depth really depends on the HHIC equipment. [16-20] In order to find out how the thickness affect the ELD process, we tested four PMETAC coatings with thickness of 9.9 nm, 26.8 nm, 42.7 nm and 64.5 nm, which were obtained by spin coating solutions with concentration of 2.5 mg/mL, 5.0 mg/mL, 7.5 mg/mL, and 10.0 mg/mL, respectively. After 120 s of HHIC exposure and 10 min of ELD, it was found that Cu films were formed on all these surfaces except that with the thickest PMETAC coating, 64.5 nm. In other word, it means that the PMETAC was not successfully grafted when the initial coating is 64.5 nm, but it was successful when the coating is 42.7 nm or less. For the coating of 64.5 nm, the grafting did not work even when the HHIC treatment time was increased to 600 s. That suggests that the cross-linking depth of PMETAC by HHIC cannot go deeper than 64.5 nm for the HHIC equipment in our lab. Thus, the initial PMETAC layer before HHIC exposure should not be thicker than 45 nm to ensure that the PMETAC is properly grafted to PET, this gives a very important reference to the printing process. While too thin a layer is not desirable either. As observed by AFM, when the initial PMETAC coating is 9.9 nm, the resultant PMETAC-PET is not as uniform (Fig. 39) compared with layers of 26.8 nm (Fig. 35) and 42.7 nm (Fig. 40). As Fig. 41 shows, after 10 min of ELD, the Cu film obtained on the thinnest PMETAC-PET surface has the biggest variation in thickness, indicating poor uniformity. Moreover, the thicker of the PMETAC coating before HHIC exposure, the thicker the resultant metal film after the same time of ELD, because the thicker PMETAC grafted on the surface offers more uptake of $PdCl_4^{2-}$ moieties, resulting in faster deposition of Cu on surface.

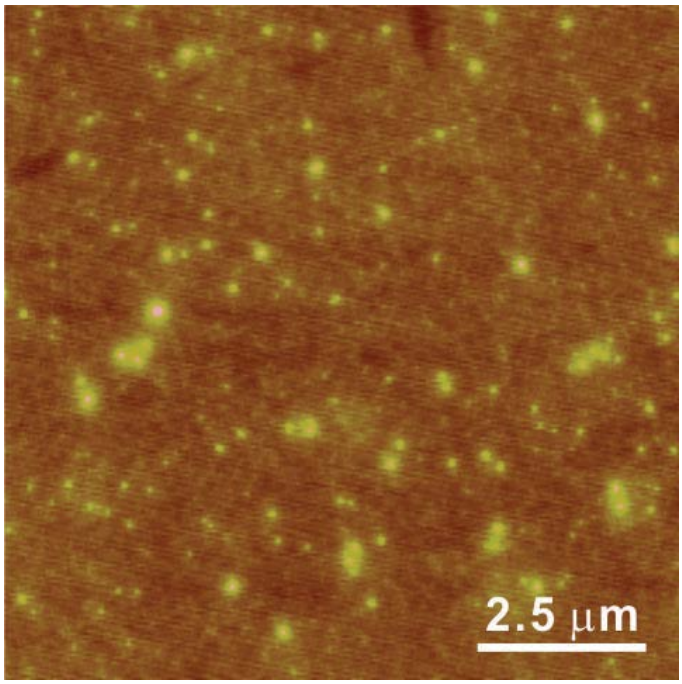

Figure 39: AFM image of PMETAC-PET obtained on 9.9 nm thick coating

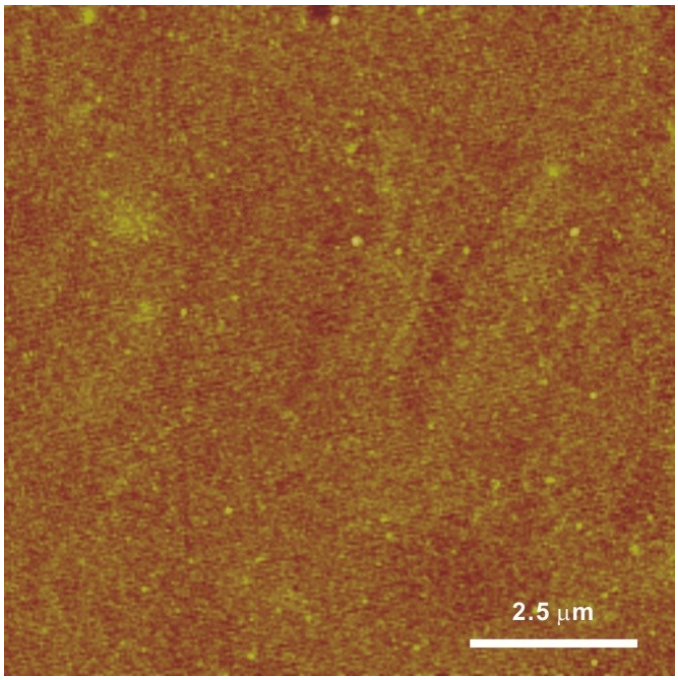

Figure 40: AFM image of PMETAC-PET obtained by HHIC exposure on 42.7 nm-thick PMETAC coating. The Z-scale is 100 nm

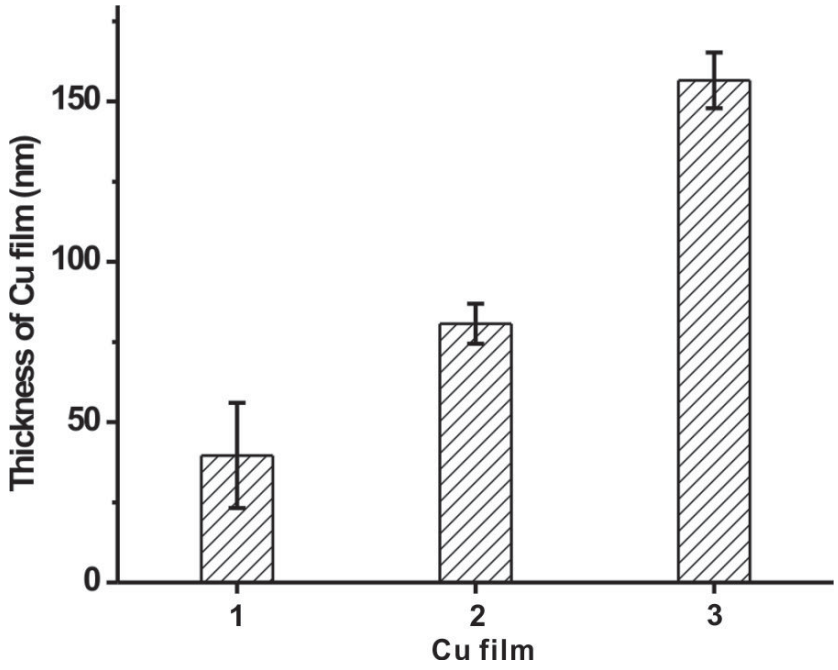

Figure 41: Thickness of Cu films obtained at 10 min of ELD on PMETAC-PET surfaces based on PMETAC coating with initiate thickness of 9.9 nm, 26.8 nm, and 42.7 nm before HHIC exposure

Typically, for this polyelectrolytes grafted surface, longer ELD plating time results in thicker Cu films. As shown in Fig. 42, thickness of the resultant Cu film is proportional to the ELD time. 30 min of ELD plating results in c.a. 385 nm thick Cu film on PET with the deposition rate of ~13 nm per min, which agrees with that previous reported on polydimethylsiloxane (PDMS). This suggests that the polyelectrolyte grafted to PET by HHIC are as good as those grafted by the typical SI-ATRP for forming metal films by ELD. A four-probe method measurement showed that the sheet resistance of the Cu film obtained at 30 min of ELD is ~2 Ω. Its conductivity is ~4.2×10^7 S/mm, which is very close to the value of bulk copper.

More importantly, this HHIC grafting technology is compatible with patterning technologies, which are crucial for electronics applications. As a proof-of-concept

demonstration, patterned Cu lines with width of ~800 µm and high spatial resolution were prepared on PET by using a shadow mask covering the surface when exposed to hyperthermal hydrogen, followed by ion exchange and 20 min of ELD (Fig. 43). To demonstrate the flexible electronics application, one of the patterned Cu lines was integrated into a simple circuit with a 9V battery to light a light-emitting diode (LED), as shown in Fig. 43 (b). The LED maintained illumination intensity even when the copper lines were bended. Moreover, the HHIC technology is principally capable of grafting polyelectrolytes onto various hydrocarbon substrates to get metallization via ELD. For example, patterned Cu lines were also obtained on PDMS film (Fig.44), implying that the present technology has potential in stretchable electronics.

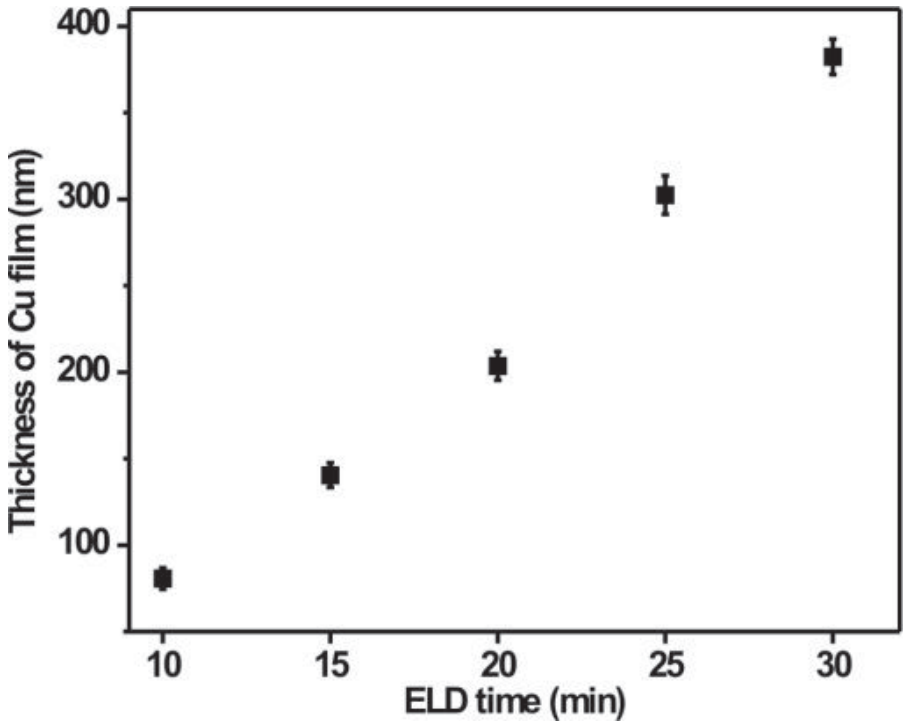

Figure 42: Thickness of Cu films as function of ELD time

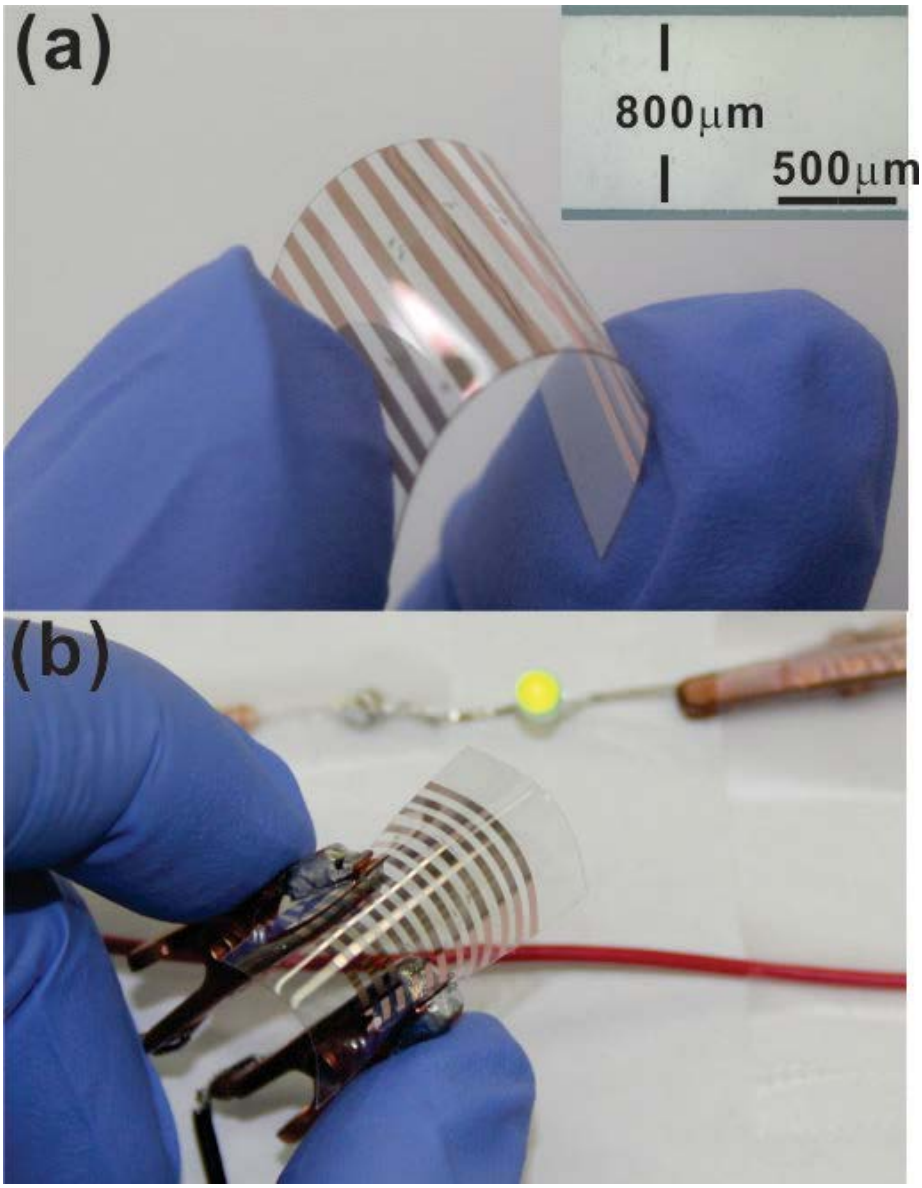

Figure 43: Photos of patterned Cu lines on PET (a) and the integrated circuit operated under bending (b)

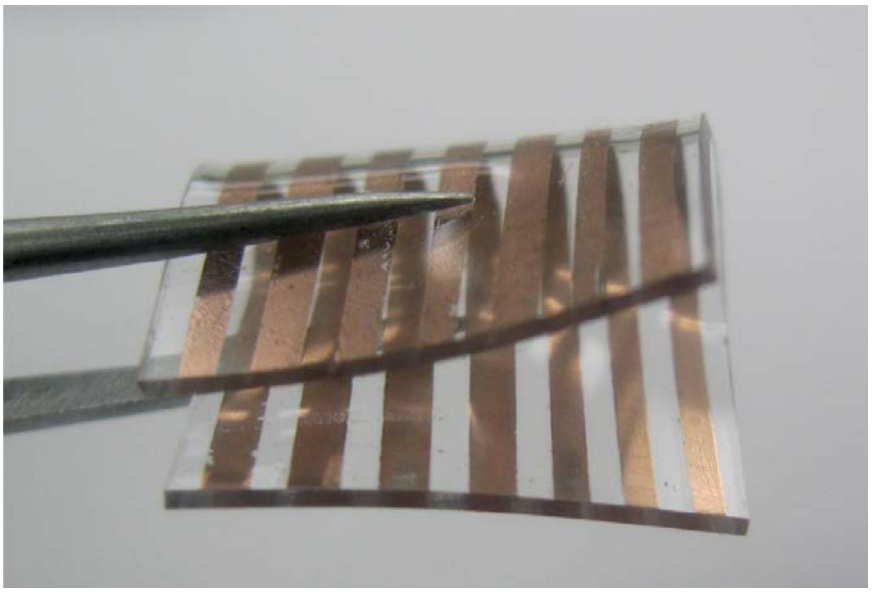

Figure 44: Patterned Cu lines on PDMS film

3.4 Conclusion

In summary, we have successfully demonstrated a physical, “green” and dry-process approach of grafting polyelectrolytes on the hydrocarbon surfaces to form metal coated polymer patterns subsequently by ELD, achieving a high quality copper patterns on PET and PDMS films. By properly controlling the hyperthermal hydrogen, PMETAC can be grafted to polymeric substrates in only a few minutes by selectively cleaving only C-H bonds to generate carbon centered radicals. Dense and uniform Cu films on various substrates were obtained by ELD catalyzed by Pd moieties loaded on the grafted polyelectrolytes. The Cu films had excellent adhesion to substrates and competitive conductivity close to bulk copper (70%). These results suggest that the present HHIC grafting technology is a promising approach for metalizing polymeric materials

containing C-H bonds, which could have potential applications in the emerging flexible and stretchable printed electronics industry.

3.5 References

[1] J. A. Rogers, T. Someya, and Y. Huang, "Materials and mechanics for stretchable electronics," *Science,* vol. 327, pp. 1603-1607, 2010.

[2] K. L. Mittal, *Metallized Plastics 7: Fundamental & Applied Aspects*: Vsp, 2001.

[3] O. Azzaroni, Z. J. Zheng, Z. Q. Yang, and W. T. S. Huck, "Polyelectrolyte brushes as efficient ultrathin platforms for site-selective copper electroless deposition," *Langmuir,* vol. 22, pp. 6730-6733, Aug 1 2006.

[4] X. Liu, X. Zhou, Y. Li, and Z. Zheng, "Surface-grafted polymer-assisted electroless deposition of metals for flexible and stretchable electronics," *Chem Asian J,* vol. 7, pp. 862-70, May 2012.

[5] X. Q. Liu, H. X. Chang, Y. Li, W. T. S. Huck, and Z. J. Zheng, "Polyelectrolyte-Bridged Metal/Cotton Hierarchical Structures for Highly Durable Conductive Yarns," *Acs Applied Materials & Interfaces,* vol. 2, pp. 529-535, Feb 2010.

[6] X. Wang, H. Hu, Y. Shen, X. Zhou, and Z. Zheng, "Stretchable conductors with ultrahigh tensile strain and stable metallic conductance enabled by prestrained polyelectrolyte nanoplatforms," *Advanced Materials,* vol. 23, pp. 3090-4, Jul 19 2011.

[7] A. Garcia, T. Berthelot, P. Viel, A. Mesnage, P. Jegou, F. Nekelson, *et al.*, "ABS Polymer Electroless Plating through a One-Step Poly(acrylic acid) Covalent Grafting," *Acs Applied Materials & Interfaces,* vol. 2, pp. 1177-1183, Apr 2010.

[8] A. Garcia, T. Berthelot, P. Viel, J. Polesel-Maris, and S. Palacin, "Microscopic Study of a Ligand Induced Electroless Plating Process onto Polymers," *Acs Applied Materials & Interfaces,* vol. 2, pp. 3043-3051, Nov 2010.

[9] A. Garcia, J. Polesel-Maris, P. Viel, S. Palacin, and T. Berthelot, "Localized Ligand Induced Electroless Plating (LIEP) Process for the Fabrication of Copper Patterns Onto Flexible Polymer Substrates," *Advanced Functional Materials,* vol. 21, pp. 2096-2102, Jun 7 2011.

[10] W. H. Yu, Y. Zhang, E. T. Kang, K. G. Neoh, S. Y. Wu, and Y. F. Chow, "Electroless plating of copper via a Sn-free process on dielectric SiLK surface modified by UV-induced graft copolymerization with 4-vinylpyridine and 1-vinylimidazole," *Journal of the Electrochemical Society,* vol. 149, pp. C521-C528, Oct 2002.

[11] Y. Q. Zhu, E. T. Kang, K. G. Neoh, T. Osipowicz, and L. Chan, "Plasma graft copolymerization of 4-vinylpyridine on dense and porous SiLK for electroless plating of copper and for retardation of copper diffusion," *Journal of the Electrochemical Society,* vol. 152, pp. F107-F114, 2005.

[12] W. C. Wang, R. K. H. Vora, E. T. Kang, and K. G. Neoh, "Electroless plating of copper on fluorinated polyimide films modified by plasma graft copolymerization and UV-induced graft copolymerization with 4-vinylpyridine," *Macromolecular Materials and Engineering,* vol. 288, pp. 152-163, Feb 20 2003.

[13] J. S. Wang and K. Matyjaszewski, "Controlled Living Radical Polymerization - Halogen Atom-Transfer Radical Polymerization Promoted by a Cu(I)Cu(Ii) Redox Process," *Macromolecules,* vol. 28, pp. 7901-7910, Nov 6 1995.

[14] F. Zhou, W. M. Shu, M. E. Welland, and W. T. S. Huck, "Highly reversible and multi-stage cantilever actuation driven by polyelectrolyte brushes," *Journal of the American Chemical Society,* vol. 128, pp. 5326-5327, Apr 26 2006.

[15] Y. Liu, D. Q. Yang, H. Y. Nie, W. M. Lau, and J. Yang, "Study of a hydrogen-bombardment process for molecular cross-linking within thin films," *Journal of Chemical Physics,* vol. 134, Feb 21 2011.

[16] Z. Zheng, W. M. Kwok, and W. M. Lau, "A new cross-linking route via the unusual collision kinematics of hyperthermal protons in unsaturated hydrocarbons: the case of poly(trans-isoprene)," *Chem Commun (Camb),* pp. 3122-4, Aug 7 2006.

[17] Z. Zheng, K. W. Wong, W. C. Lau, R. W. Kwok, and W. M. Lau, "Unusual kinematics-driven chemistry: cleaving C-H but not COO-H bonds with hyperthermal protons to synthesize tailor-made molecular films," *Chemistry,* vol. 13, pp. 3187-92, 2007.

[18] Z. Zheng, X. Xu, X. Fan, W. M. Lau, and R. W. Kwok, "Ultrathin polymer film formation by collision-induced cross-linking of adsorbed organic molecules with hyperthermal protons," *J. Am. Chem. Soc.,* vol. 126, p. 12336, 2004.

[19] C. V. Bonduelle, W. M. Lau, and E. R. Gillies, "Preparation of protein- and cell-resistant surfaces by hyperthermal hydrogen induced cross-linking of poly(ethylene oxide)," *ACS Appl Mater Interfaces,* vol. 3, pp. 1740-8, May 2011.

[20] D. B. Thompson, T. Trebicky, P. Crewdson, M. J. McEachran, G. Stojcevic, G. Arsenault, *et al.*, "Functional Polymer Laminates from Hyperthermal Hydrogen Induced Cross-Linking," *Langmuir,* vol. 27, pp. 14820-14827, Dec 20 2011.

[21] C. V. Bonduelle, W. M. Lau, and E. R. Gillies, "Preparation of Protein-and Cell-Resistant Surfaces by Hyperthermal Hydrogen Induced Cross-Linking of Poly (ethylene oxide)," *ACS applied materials & interfaces,* vol. 3, pp. 1740-1748, 2011.

[22] Q. Ye, X. L. Wang, H. Y. Hu, D. A. Wang, S. B. Li, and F. Zhou, "Polyelectrolyte brush templated multiple loading of Pd Nanoparticles onto TiO2 nanowires via regenerative counterion exchange-reduction," *J. Phys. Chem. C*, vol. 113, p. 7677, 2009.

[23] X. Wang, Z. Feng, and W. Liu, "Effects of atomic oxygen and ultraviolet in low earth orbit on low surface energy polymer film," *Journal of Applied Polymer Science*, vol. 120, pp. 329-334, 2011.

Chapter 4

4 Summary and future work

4.1 Summary

Motivation of this thesis work lies in pushing forward the board of the printed electronics by solving those critical issues which are preventing the development of the printed electronics industry. Printing technology for flexible electronics is a strategic topic globally. The majority of the market is growing rapidly enabled by the use of flexible or stretchable electronics. Electronic devices and system to be fabricated on flexible substrates are the subjects of growing attention within both the research and industrial community. Printed electronics is a technical trend to realize low-power, inexpensive in electronics industry. In addition, portable printing technology will become a popular method of making modular electronics, which is a growing tendency for electronics industry.

In chapter 1, we proposed a new method of fabricating copper based printed electronics with high conductivity and high resolution on flexible photopaper substrate, successfully achieving objective 1. Instead of directly printing metal nano-particles (silver, copper, copper oxide, etc.), we used a palladium salt based ink as our deposition material, eliminating many critical issues such as nozzle clog and misdirected jetting which are caused by the accumulation of the nanoparticles at the nozzle opening. Thickness of the printed metal is also a critical problem in this area, since the single pulse jetting volume is limited (to keep a high printing resolution), it's impossible for conventional inkjet printing technique to create metal layer with a satisfied thickness, which caused the low

conductivity of the printed pattern. Though they may have a conductivity value which is close to the bulk material (usually 30% in this area), the resistance is still huge since the metal layer is too thin. In our method, we printed the pattern with “seed” ink which served as the catalyst in the following ELD process. During the ELD process, copper ions in the solution were reduced on the surface of the pattern, forming a dense, thick, and uniform copper layer on the substrate with high conductivity and high resolution.

However, photopaper is easy to be damaged, though it is environmentally friendly. For some applications, photopaper is absolutely qualified, such as RFID tag, smart label and circuits’ board which are not intended to work in the extreme condition. But for some other applications, such as flexible display, devices that work under water and solar panel which needs to work under the sunlight for a long time, a paper based electronics will never be the first choice. So we set our next goal --- making the high conductivity, high resolution copper based printed electronics on polymer based substrate, which is demonstrated in chapter 3.

Different from paper which can easily “absorb” chemical solutions, the polymer based substrate is chemical inert. Conventional wet chemical surface treatment method takes long time and large amount of money to get such substrate well treated for strong adhesion printing. So in chapter 3 we focused on a new surface treatment method to graft polyelectrolyte onto the targeted substrate and a physical, “green” and dry-process approach of grafting polyelectrolytes on the hydrocarbon surfaces to form metal coated polymer patterns subsequently by ELD, achieving a high quality copper patterns on PET and PDMS films is developed. By properly controlling the hyperthermal hydrogen, PMETAC can be grafted to polymeric substrates in only a few minutes by selectively

cleaving only C-H bonds to generate carbon centered radicals. Copper patterns fabricated using this method a satisfied thickness (~380 nm) and a high conductivity (~70% bulk). Objective 2 was achieved and we pushed the board of the printed electronics forward again.

4.2 Thesis contributions

This thesis proposed a new method of fabricating copper based flexible printed electronics, overcoming many critical issues faced by nowadays printed electronics industry. The success of the project with high potential to be scaled to economically and industrially relevant production level, which will help the development of electronics manufacturing technologies and industry in Canada and all around the world. In order to accelerate the transfer of research results into industrial applications, the development of robust, high-resolution, high-performance and low-cost printing technologies will play a pivotal role.

4.3 Future work

Based on our established expertise and previous studies, our future work will focus on the following aspects:

1. Fabrication of multi-layer metallic circuits on polyelectrolyte modified paper by printing noble-metal-containing salt solution (catalyst) followed by electroless deposition (ELD) of Cu or Ni;

2. Fabrication of multi-layer metallic circuits on polymer films by printing polyelectrolyte on hydrocarbon polymeric films followed by grafting via

hyperthermal hydrogen induced cross-linking (HHIC) and electroless deposition of Cu or Ni;

3. Fabrication of stretchable circuits by material printing conductive materials on fluorinated surface followed by a replication method;

4. Study of the structure-property-function relationships of the printed flexible conductors on various substrate materials;

5. Development of various applications of flexible and stretchable electronics/devices, including strain, pressure and touch sensors, paper based RFID, loudspeakers and power generators, built-in circuits, organic LED array, and all-organic thin film transistors.

The long-term goal is to develop nanoscale printer head nozzles for high-resolution material printing, fabricate nanoscale printed electronics and integrate the new material printing processes to be developed in this project into industrial scale roll-to-roll processes for mass production.

Curriculum Vitae

Name:	Tengyuan Zhang
Post-secondary Education and Degrees:	Beijing Institute of Technology Beijing, China 2008-2012 B.A.
Honors and Awards:	First prize of Chinese Renmin Scholarship 2009-2012 Capital Merit Student 2011-2012
Related Work Experience	Teaching Assistant the University of Western Ontario 2013-Present

Publications:

T. Zhang, X. Wang, T. Li, Q. Guo, and J. Yang, "Fabrication of flexible copper-based electronics with high-resolution and high-conductivity on paper via inkjet printing," Journal of Materials Chemistry C, 2013

X. Wang, X. Cai, Q. Guo, T. Zhang, B. Kobe, and J. Yang, "i3DP, a robust 3D printing approach enabling genetic post-printing surface modification," Chemical Communications, vol. 49, pp. 10064-10066, 2013.

X. Wang, T. Zhang, B. Kobe, W. M. Lau, and J. Yang, "Grafting of polyelectrolytes onto hydrocarbon surfaces by high-energy hydrogen induced cross-linking for making metallized polymer films," Chemical Communications, vol. 49, pp. 4658-4660, 2013.

T. Zhang and Y. Mei, "Automatic image registration algorithm based on improved Harris corner detection," in Proc. of SPIE Vol, 2011, pp. 82853S-1.